# *Triple-Bond Reactivity of an AsP Complex Intermediate: Synthesis Stemming from Molecular Arsenic, As-4*



**Citation:** Spinney, Heather A., Nicholas A. Piro, and Christopher C. Cummins. "Triple-Bond Reactivity of an AsP Complex Intermediate: Synthesis Stemming from Molecular Arsenic, As 4." Journal of the American Chemical Society 131.44 (2009) : 16233-16243.

**As Published:** http://dx.doi.org/10.1021/ja906550h

**Publisher:** American Chemical Society

**Persistent URL:** http://hdl.handle.net/1721.1/65118

**Version:** Author's final manuscript: final author's manuscript post peer review, without publisher's formatting or copy editing

# Triple-Bond Reactivity of an AsP Complex Intermediate: Synthesis Stemming from Molecular Arsenic, $As_4$

Heather A. Spinney, Nicholas A. Piro, and Christopher C. Cummins*

*Department of Chemistry, Massachusetts Institute of Technology, Cambridge MA 02139-4307*

*ccummins@mit.edu*

**Abstract**

While $P_4$ is the stable molecular form of phosphorus, a recent study illustrated the possibility of $P_2$ generation for reactions in organic media under mild conditions. The heavier group 15 element arsenic can exist as $As_4$ molecules, but $As_4$ cannot be stored as a pure substance because it is both light-sensitive and reverts thermally to its stable, metallic grey form. Herein we report $As_4$ activation giving rise to a $\mu$-$As_2$ diniobium complex, serving in turn as precursor to a terminal arsenide anion complex of niobium. Functionalization of the latter provides the new AsPNMes* ligand, which when complexed with tungsten pentacarbonyl elicits extrusion of the (AsP)W(CO)$_5$ molecule as a reactive intermediate. Trapping reactions of the latter with organic dienes are found to furnish double Diels-Alder adducts in which the AsP unit is embedded in a polycyclic organic framework. Thermal generation of (AsP)W(CO)$_5$ in the presence of the neutral terminal phosphide complex P≡Mo(N[$^i$Pr]Ar)$_3$ leads to the *cyclo*-$AsP_2$ complex (OC)$_5$W(*cyclo*-$AsP_2$)Mo(N[$^i$Pr]Ar)$_3$. The (AsP)W(CO)$_5$ trapping products were crystallized and characterized by X-ray diffraction methods, and computational methods were applied for analysis of the As—As and As—P bonds in the complexes.

# Introduction

Yellow arsenic (molecular $As_4$) is attractive as a soluble, molecular source of this element for chemical synthesis in solution, but its use is complicated because it readily polymerizes to the metallic grey allotrope;[1] $As_4$ is photosensitive and thermally unstable as a solid, but exhibits good thermal stability in solution and in the gas phase. Bettendorff[2] has been credited as the first to report yellow arsenic,[1] and an early discussion of arsenic allotropes was provided by Linck.[3] Stock and Siebert reported a method of $As_4$ generation using an electric arc,[4] while Erdmann and von Unruh diagrammed an $As_4$ synthesis using what is essentially a simple tube furnace.[5] Scherer et al. have utilized $As_4$ solutions prepared in that manner[6] in xylene or decalin at reflux (140 or 170 °C, respectively) for reactions with transition-metal carbonyls in syntheses of *cyclo*-$As_n$ ligands ($n = 3-6, 8$)[7] and metal-arsenic clusters.[8] Having prepared the first complexes containing ligated *cyclo*-$P_3$, Sacconi et al. reported generation of $As_4$ by the tube furnace method and its transformation to provide *cyclo*-$As_3$ as a bridging ligand.[9] West et al. also described $As_4$ activation by the disilene system $Mes_2Si{=}SiMes_2$ in toluene solution.[10] The foregoing is nearly an exhaustive summary of the known solution-phase reaction chemistry of the $As_4$ molecule. Herein we add to this body of knowledge that is derived from the tube furnace method of $As_4$ generation.[5]

In prior work we showed that the niobaziridine-hydride complex HNb($\eta^2$-$^t$BuHC=NAr)(N[Np]Ar)$_2$ (**1**, where Np = $CH_2{}^tBu$ and Ar = 3,5-$C_6H_3Me_2$; Figure 1) activates $P_4$ in organic solvents at 20 °C, and that the product of this activation is a $\mu$-$P_2$ diniobium complex.[11] We went on to show that 2e reduction of the $\mu$-$P_2$ diniobium complex elicited P—P bond cleavage with formation of a terminal phosphide anion complex, $[P{\equiv}Nb(N[Np]Ar)_3]^-$.[12] The latter has proven to be quite versatile for transfer of the phosphide phosphorus atom to various electrophiles, resulting in interesting bound ligands or free main-group species.[13] Of particular note is the functionalization of $[P{\equiv}Nb(N[Np]Ar)_3]^-$ with Niecke's chloroiminophosphane, ClP=NMes* (Mes* = 2,4,6-$C_6H_2{}^tBu_3$),[14] leading to the synthesis of a diphosphaazide complex of niobium, ($\eta^2$-PPNMes*)Nb(N[Np]Ar)$_3$, which upon thermolysis rearranges to the niobium(V) imido, (Mes*N)Nb(N[Np]Ar)$_3$, with loss of the $P_2$ molecule.[15] As represented in a series of pa-

pers, we have gathered convincing evidence for the intermediacy of the free $P_2$ molecule as a reactive transient engaging in in Diels-Alder reactions with organic dienes and undergoing addition to terminal phosphide M≡P triple bonds to yield *cyclo*-$P_3$ complexes.[15,16] Similar triple-bond reactivity has likewise been exhibited by the tungsten pentacarbonyl complex of $P_2$, having the formula $(P_2)W(CO)_5$, a species also proposed to be accessible as a reactive transient intermediate.[15–17] Accordingly, a primary aim of the present work was to investigate the $As_4$ activation chemistry of **1** in search of parallels with the prior line of inquiry based on $P_4$ activation.

A second aim of the present work was to discover if our established scheme for $P_2$ generation/transfer could be extended to provide access to the diatomic molecule AsP, either in free form or else stabilized as its tungsten pentacarbonyl complex. In the gas-phase phosphorus-arsenic system at 600-850 °C, it has been shown that the major species present are the tetrahedral molecules $As_nP_{4-n}$ ($n = 1-4$; a selective, low-temperature route to $AsP_3$ was reported recently[18]), but that the diatomic molecule AsP is also present as a significant percentage of the mixture and plays an important role in the system.[19] In contrast, the homonuclear diatomic molecules $P_2$ and $As_2$ have negligible concentration at these temperatures. An AsP solid solution phase has also been described for the arsenic-phosphorus system under the high-pressure conditions needed to suppress sublimation of the elements near 600 °C.[20] Vibrational signatures for the AsP molecule were first observed using a microwave discharge through a flowing mixture of $AsCl_3$ and $PCl_3$,[21] and the molecule has been generated more recently by laser ablation of arsenic in the presence of $PH_3$.[22] AsP has a measured dissociation energy of $429.7 \pm 12.6$ kJ mol$^{-1}$,[23] and an equilibrium bond distance of 1.9995440(2) Å.[22] Bimetallic complexes containing bridging AsP ligands have been synthesized by treating the salts $[Li][M_2Cp_2(CO)_4(\mu\text{-}PH_2)]$ (M = Mo, W) with an equivalent of $AsCl_3$;[24] however, no investigations of AsP triple-bond reactivity under preferred conditions for solution-phase organic reactions (25 °C, 1 atm) have been described.

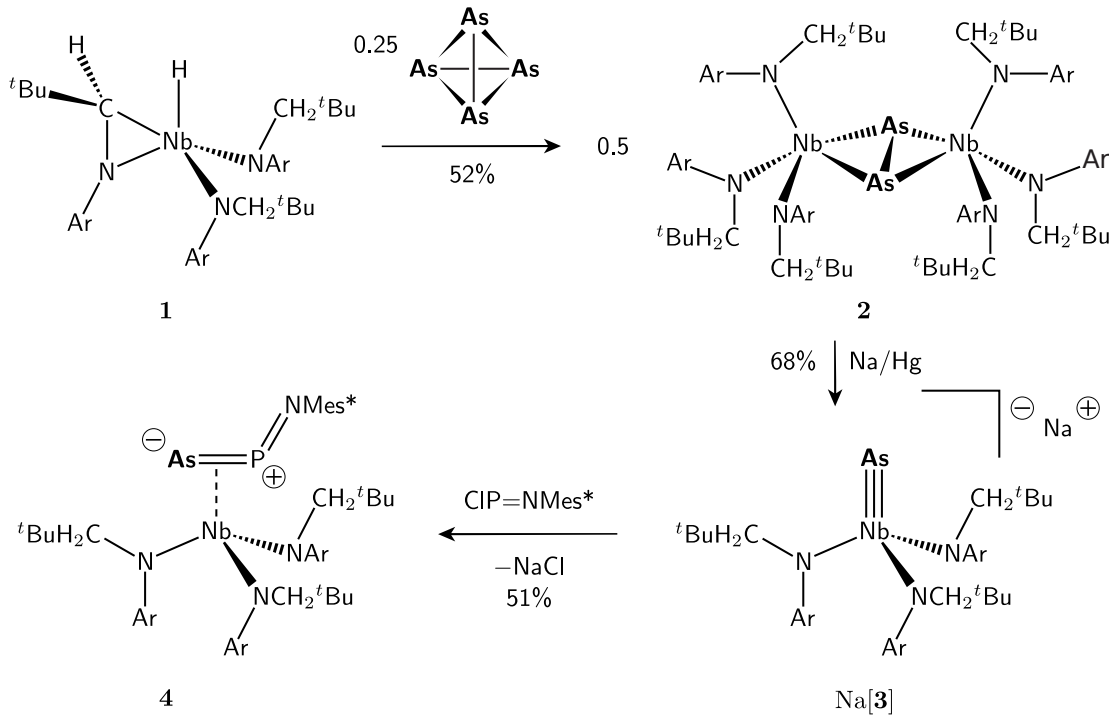


Figure 1: Three-step synthesis of the $\eta^2$-AsPNMes* complex **4** in a sequence encompassing $As_4$ activation, $\mu$-$As_2$ ligand reductive cleavage, and terminal arsenide functionalization with the $[PNMes^*]^+$ electrophile.

# Results and discussion

## Reaction of Niobaziridine Hydride with $As_4$

To a cold (−30 °C) solution of $As_4$ in toluene was added niobaziridine-hydride complex **1** *via* a solid addition tube, and then the reaction mixture was allowed to warm to room temperature in the dark (Figure 1). After stirring for 16 h, it was observed that the reaction mixture had attained a dark green color, indicative of $\mu$-$As_2$ complex ($\mu_2$:$\eta^2$,$\eta^2$-$As_2$)[Nb(N[Np]Ar)$_3$]$_2$, **2**. Diarsenide complex **2** was then isolated as a bright green powder in 52% yield. A single-crystal X-ray diffraction study of complex **2** has not yet resulted in a high quality structure solution, but one study did confirm the connectivity proposed for the molecule as drawn (Figure 1).

The most important structural parameter for complex **2** is the As—As interatomic distance, so the model system ($\mu_2$:$\eta^2$,$\eta^2$-$As_2$)[Nb(N[Me]Ph)$_3$]$_2$ was constructed and subjected to geometry optimization using density functional theory (DFT) methods to obtain $r_{\mathrm{As—As}}$ (calcd.) = 2.365 Å. In the activation of $As_4$ by niobaziridine-hydride complex **1**, a rare example is generated of a molecule containing an $M_2As_2$ butterfly core. The only structurally-characterized prior examples of such a molecule are ($\mu$-$As_2$)[Mn(CO)$_2$Cp*]$_2$[25] and ($\mu$-$As_2$)[Pd(PPh$_3$)$_2$]$_2$,[26] which have interarsenic distances of 2.225(1) and 2.274(1) Å, respectively. A related structural type is represented by the complex [AsMoCp′(CO)$_2$]$_2$ (Cp′ = $^i$PrC$_5$H$_4$),[27] in which there exists a Mo—Mo bond and the central $As_2Mo_2$ unit is an approximate tetrahedron with $r_{\mathrm{As—As}}$ = 2.302(1) Å. The single-bond covalent radius for As is 1.21 Å,[28] while the double-bond covalent radius is 1.14 Å.[29] As such, As—As bonds are expected to be ca. 2.42 Å long, while As=As bonds are expected to be ca. 2.28 Å long, and based on the crystallographic data for the diarsane (Mes)$_2$As—As(Mes)$_2$ (2.472(3) Å)[30] and the diarsene Mes*As=AsMes* (2.2634(3) Å),[31] these are indeed acceptable values. By these criteria, our complex **2** (calculated $r_{\mathrm{As—As}}$ = 2.365 Å) might be assigned some As—As double bond character. To assess this in more detail, we turned to a topological analysis of the calculated electron density; calculated properties for several molecules from the present work as well as for some reference molecules are collected in Table 1. Consideration of the electron

density $\rho_b$ at the As—As bond critical point for our model system representing **2** gives a bond order $n$ = 1.14 (Table 1). This is consistent with the representation of **2** as drawn in Figure 1 with an interarsenic single bond. These values compare well with those calculated similarly for the spherical-aromatic[32] $As_4$ molecule: $r_{As—As}$ = 2.4372 Å (exp. = 2.44 Å[33]).

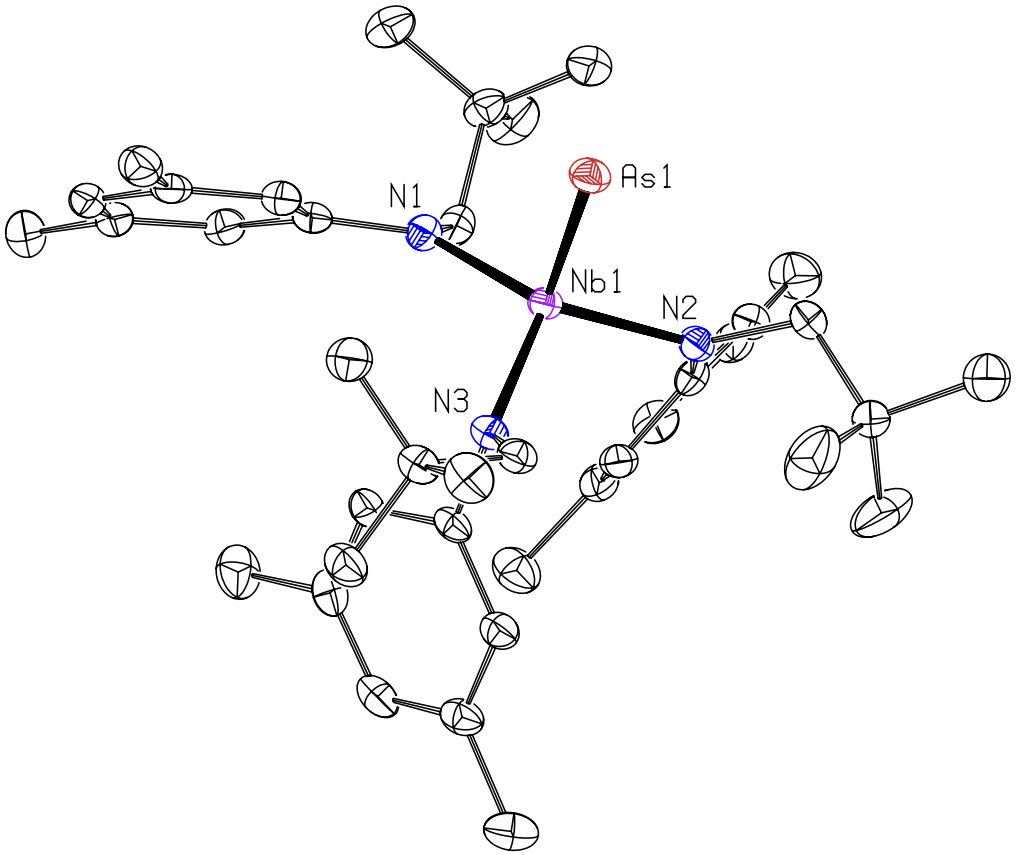


Figure 2: Molecular structure of anion **3** as found in crystals of the salt [Na(12-crown-4)$_2$][As≡Nb(N[Np]Ar)$_3$] shown with 50% probability thermal ellipsoids. Selected interatomic distances (Å) and angles (°): Nb1–As1, 2.3078(5); Nb1–N1, 2.107(2); Nb1–N2, 2.058(2); Nb1–N3, 2.051(2); As1–Nb1–N1, 108.10(7); As1–Nb1–N2, 103.48(7); As1–Nb1–N3, 100.89(7).

## Terminal Arsenide Anion Synthesis

Two-electron reduction of diarsenide **2** was achieved by treatment with an excess of 1% Na/Hg in tetrahydrofuran (THF) solvent. This led to the isolation in 68% yield of the $[Na(THF)]^+$ salt of the arsenide complex anion $[As{\equiv}Nb(N[Np]Ar)_3]^-$, **3**, which was found to crystallize as a close-

Table 1: Topological Properties of Selected As—As and As—P Bonds

| Molecule[a] | Distance[b] | $\rho_b$[c] | $n$[d] | $\nabla^2\rho$[e] | $\varepsilon$[f] | $q_{\mathrm{As}}$[g] | $q_{\mathrm{P}}$[g] |
|---|---|---|---|---|---|---|---|
| $As_2$ | 2.108 | 0.134 | 3.00 | −0.042 | 0.00 | 0.00 | |
| *E*-HAs=AsH | 2.255 | 0.110 | 2.00 | −0.056 | 0.33 | +0.31 | |
| $H_2AsAsH_2$ | 2.482 | 0.081 | 1.00 | −0.043 | 0.00 | +0.51 | |
| $As_4$ | 2.437 | 0.079 | 1.03 | −0.003 | 0.07 | +0.00 | |
| AsP | 2.006 | 0.153 | 3.00 | −0.139 | 0.00 | +0.10 | −0.10 |
| *E*-HAs=PH | 2.155 | 0.125 | 2.00 | −0.110 | 0.33 | +0.35 | +0.37 |
| $H_2AsPH_2$ | 2.366 | 0.094 | 1.00 | −0.071 | 0.03 | +0.55 | +0.86 |
| $AsP_3$ | 2.324 | 0.091 | 1.04 | −0.015 | 0.11 | +0.17 | −0.06 |
| ($\mu$-$As_2$)[Nb(N[Me]Ph)$_3$]$_2$ | 2.364 | 0.084 | 1.14 | +0.009 | 0.36 | −0.53 | |
| ($\eta^2$-AsPNMes)Nb(N[Me]Ph)$_3$ | 2.138 | 0.120 | 1.72 | −0.048 | 0.06 | −0.25 | +0.67 |
| (AsP[PW(CO)$_5$])Mo(N[Me]Ph)$_3$[h] | 2.328 | 0.090 | 1.03 | −0.013 | 0.14 | −0.00 | −0.21 |
| | 2.244 | 0.103 | 1.28 | −0.041 | 0.02 | −0.00 | −0.37 |
| (As[PW(CO)$_5$])($C_6H_8$)$_2$ | 2.297 | 0.106 | 1.35 | −0.088 | 0.04 | +0.52 | +0.36 |

[a] All molecules geometry-optimized without symmetry constraints at the spin-restricted all-electron OLYP ZORA level of theory with QZ4P basis for As, P, Nb, TZ2P basis for C, N, W, and O and DZP basis for H atoms.

[b] Distances given in Å.

[c] Electron density in $e/a_\circ$ at the (3, −1) As–As or As–P bond critical point.

[d] Bond order $n$ according to the definition $n = exp(A \times (\rho_b - B))$. For As–As bonds, $A = 19.7363$ and $B = 0.0774921$ as determined by least-squares fitting using $As_2$, *E*-HAs=AsH, and $H_2AsAsH_2$ as reference compounds for triple, double, and single bonds, respectively. For As–P bonds, $A = 17.23$ and $B = 0.088469$ using AsP, *E*-HAs=PH, and $H_2AsPH_2$ as reference systems.

[e] The value of the Laplacian of the electron density at the (3, −1) As–As or As–P bond critical point in $e/a_\circ^5$.

[f] Ellipticity at the (3, −1) As–As or As–P bond critical point.

[g] Atomic charge obtained by integration of the electron density over the respective As or P atomic basin.

[h] The first line of data refers to the As–P bond involving the P atom that is *not* ligated by $W(CO)_5$.

contact ion-paired dimer by X-ray diffraction analysis ($r_{As—Nb}$ = 2.3106(3) Å).[34] Also isolated and structurally characterized was the $[Na(12\text{-crown-}4)_2]^+$ salt of anion **3**, and in this case there are no close contacts involving the one-coordinate As atom of the terminal arsenide anion ($r_{As—Nb}$ = 2.3078(5) Å, see Figure 2).

Terminal arsenide complexes–characterized by one-coordinate As that is triply bonded to a metal atom–are rare, but known examples include the triamidoamine-supported complexes As≡Mo-$[(Me_3SiNCH_2CH_2)_3N]$ ($r_{As—Mo}$ = 2.252(3) Å)[35] and As≡W$[(Me_3SiNCH_2CH_2)_3N]$ ($r_{As—W}$ =-2.2903(11) Å).[36] Unlike the niobium arsenide **3**, the latter two complexes were not prepared *via* $As_4$ activation chemistry, but by treatment of the corresponding metal chloride compounds with lithium organoarsenide salts. A series of transition-metal Zintl phases containing one-coordinate As atoms (e.g., $[Cs_7][As(InAs)_3Nb{\equiv}As]$, $r_{As—Nb}$ = 2.390(2) Å) have also been reported,[37] and these represent the only instances other than our new complex **3** in which a metal terminal arsenide is also a component of an anion. For our purposes, this feature is expected to facilitate functionalization of the terminal arsenide unit.

To model the structure and bonding in anion **3**, the structure of anion $[As{\equiv}Nb(N[Me]Ph)_3]^-$ was geometry optimized with no counterion giving rise to a calculated $r_{As—Nb}$ = 2.295 Å. This agrees well with the values observed in both the $[Na(12\text{-crown-}4)_2]^+$ salt of anion **3** ($r_{As—Nb}$ = 2.3078(5) Å) and the close-contact ion-paired dimer ($r_{As—Nb}$ = 2.3106(3) Å) , and suggests that cation-anion interactions do little to perturb the strong Nb—As bond. Addition of the triple-bond covalent radii for Nb (1.16 Å) and As (1.06 Å) gives a predicted value for a Nb≡As bond of 2.24 Å,[38] while similar addition of the double-bond covalent radii gives a predicted value for a Nb=As bond of 2.39 Å.[29] Thus we can conclude that the Nb—As bond in $[As{\equiv}Nb(N[Np]Ar)_3]^-$, **3**, contains significant triple bond character.

## Preparation of the As=P=NMes* Complex

Functionalization of the terminal As atom in **3** was achieved by treatment of its $[Na(THF)]^+$ salt with the phosphorus electrophile[14] ClP=NMes* (Figure 1). This provided the desired complex,

formulated as ($\eta^2$-AsPNMes*)Nb(N[Np]Ar)$_3$, **4**. After separation from NaCl, complex **4** was isolated in 51% yield as an orange-red solid. A spectroscopic signature of complex **4** is a $^{31}$P NMR singlet at $\delta$ = 348 ppm (benzene-$d_6$, 20 °C). For comparison, the corresponding central phosphorus atom in diphosphaazide complex ($\eta^2$-PPNMes*)Nb(N[Np]Ar)$_3$ resonates at $\delta$ = 335 ppm.[15] X-ray diffraction analysis (Figure 3) revealed arsaphosphaazide complex **4** to be nearly isostructural with the diphosphaazide complex reported previously, with the AsPNMes* ligand coordinated in an $\eta^2$ fashion to niobium *via* its terminal AsP moiety. The As—P and P—N bond distances in **4** ($r_{\text{As—P}}$ = 2.1296(6) Å, $r_{\text{P—N}}$ = 1.564(2) Å) are essentially identical in length to those reported in the phosphaarsene (Me$_3$Si)$_2$HCAs=PMes* ($r_{\text{As—P}}$ = 2.124(2) Å)[39] and the iminophosphane (Me$_3$Si)$_3$CP=NMes* ($r_{\text{P—N}}$ = 1.566(3) Å),[40] and as such the AsPNMes* ligand is best represented as a heterocumulene containing As—P and P—N double bonds. A geometry optimization performed on the model compound ($\eta^2$-AsPNMes*)Nb(N[Me]Ph)$_3$ gave a calculated $r_{\text{As—P}}$ = 2.138 Å and a topological analysis performed on the same molecule gave an As—P bond order $n$ = 1.72 (Table 1). A plot of the Laplacian of the electron density for the model system for **4** is shown in Figure 4. The plot is in a plane defined by the Nb, As, and P nuclei and accumulation of valence-shell charge between P and As, as well as P and Nb, is clearly visible. The arsaphosphaazide ligand, AsPNMes*, is a new addition to a small group of heavy azide analogues,[41,42] which also includes the diphosphaazide liand, PPNMes*.

## Thermolysis of the As=P=NMes* Complex with Conversion to a Niobium Imido Complex

Thermolysis of complex **4** was carried out under various conditions. Simple thermolysis in benzene-$d_6$ solution (60 °C, 3 h) gave near quantitative conversion to the known imido complex (Mes*N)Nb(N[Np]Ar)$_3$, **5**, a molecule differing in its chemical formula from that of precursor **4** by only the AsP diatomic unit. An observed kinetic parameter for the first-order disappearance of **4** (benzene-$d_6$, 60 °C) is the rate constant $k = 2.9(1) \times 10^{-4}$ s$^{-1}$. Under these conditions, the $^{31}$P NMR signal for starting **4** was observed to decay away, while no new $^{31}$P NMR resonances were observed to

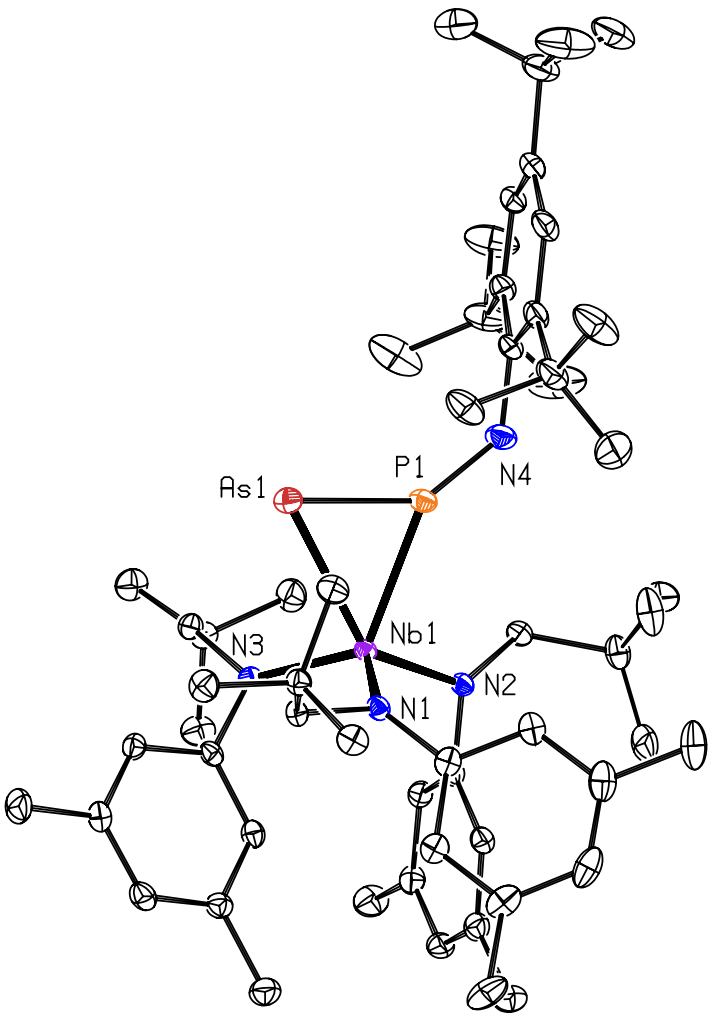


Figure 3: Molecular structure of complex **4** shown with 50% probability thermal ellipsoids. Selected interatomic distances (Å) and angles (°): As1–P1, 2.1296(6); P1–N4, 1.564(2); Nb1–As1, 2.6704(3); Nb1–P1, 2.4799(6); As1–P1–N4, 140.56(8); As1–P1–Nb1, 70.335(19); Nb1–As1–P1, 60.989(17).

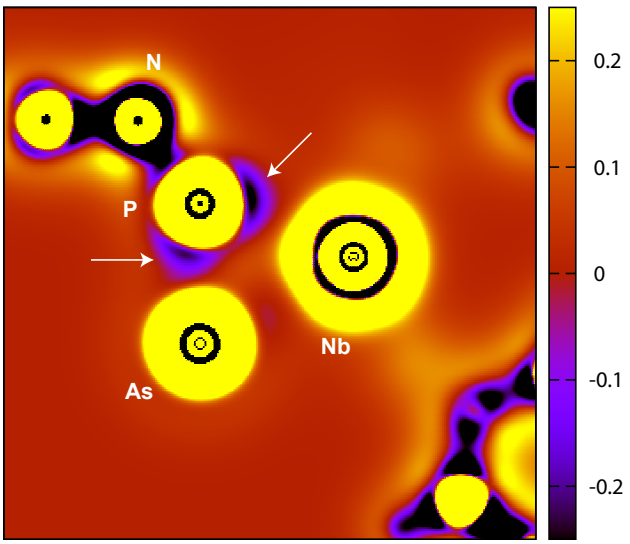


Figure 4: Plot of the Laplacian of the electron density in units of $e/a_\circ^5$ for the model system of **4**, ($\eta^2$-AsPNMes)Nb(N[Me]Ph)$_3$; the plot is in a plane defined by the Nb, As, and P nuclei. Two small arrows indicate areas of valence-shell charge concentration in the P—Nb and P—As bonding regions.

grow in.

Thermolysis of **4** (65 °C, 3 h) in neat 1,3-cyclohexandiene or neat 2,3-dimethyl-1,3-butadiene did not lead to efficient AsP trapping. The $^{31}$P NMR spectra of the reaction mixtures showed disappearance of starting material and formation of a multitude of phosphorus-containing products. Attempts to isolate individual compounds from the mixtures were unsuccessful. Resonances at $\delta$ = −79 ppm (1,3-cyclohexadiene) and $\delta$ = −52 ppm (2,3-dimethyl-1,3-butadiene) were tentatively assigned to the double Diels-Alder adducts of AsP with the respective dienes based on the corresponding shifts for the $P_2$ adducts, $P_2(C_6H_8)_2$ ($\delta$ = −80 ppm) and $P_2(C_6H_{10})_2$ ($\delta$ = −52 ppm).[15] Integration of these $^{31}$P NMR resonances versus an internal standard ($PPh_3$) revealed that the proposed AsP trapping products, $AsP(C_6H_8)_2$ and $AsP(C_6H_{10})_2$, were formed in 16% and 19% yields, respectively.[43]

We have discovered previously that M≡P bonds are more effective traps for the $P_2$ molecule than are organic dienes, and react with $P_2$ in a one-to-one fashion to form *cyclo*-$P_3$ metal complexes.[16] As such, **4** was also thermolyzed in benzene in the presence of P≡Mo(N[$^i$Pr]Ar)$_3$,

**6**,[44] with the goal of trapping AsP to form a *cyclo*-$AsP_2$ molybdenum complex (Figure 5). The As=P=NMes* complex **4** and the molybdenum phosphide **6** do not react upon mixing at room temperature; however, following completion of thermolysis (70 °C, 3 h) two new singlets appeared in the $^{31}P$ NMR spectrum at $\delta = -137$ and $\delta = -185$ ppm. The former is assigned to the new complex (*cyclo*-$AsP_2$)Mo(N[$^i$Pr]Ar)$_3$, **7**, while the latter is assigned to the previously reported complex (*cyclo*-$P_3$)Mo(N[$^i$Pr]Ar)$_3$, which has been prepared both *via* thermolysis of the diphosphaazide complex ($\eta^2$-PPNMes*)Nb(N[Np]Ar)$_3$ in the presence of **6**[16] and *via* $P_4$ activation by Mo(H)($\eta^2$-$Me_2$C=NAr)(N[$^i$Pr]Ar)$_2$.[45] Monitoring formation of **7** by $^{31}P$ NMR ($PPh_3$ as internal standard) gave an overall yield of 10% for the *cyclo*-$AsP_2$ compound, compared to 20% for the *cyclo*-$P_3$ compound. The mixture of (*cyclo*-$E_3$)Mo(N[$^i$Pr]Ar)$_3$ complexes was separated from the (Mes*N)Nb(N[Np]Ar)$_3$ coproduct, **5**, by dissolving the crude solids from the reaction mixture in $Et_2O$ and cooling the solution to −35 °C, whereupon white, fibrous crystals of the (*cyclo*-$E_3$)Mo(N[$^i$Pr]Ar)$_3$ complexes precipitated. The (*cyclo*-$AsP_2$)Mo(N[$^i$Pr]Ar)$_3$, **7**, and (*cyclo*-$P_3$)Mo(N[$^i$Pr]Ar)$_3$ compounds are indistinguishable by $^1H$ and $^{13}C$ NMR spectroscopy; only one set of resonances for the anilide ligands was observed when the mixture of the two compounds was dissolved in THF-$d_8$. Further attempts to separate **7** and (*cyclo*-$P_3$)Mo(N[$^i$Pr]Ar)$_3$ by fractional crystallization were unsuccessful.

The only reported example of a *cyclo*-$AsP_2$ complex in the literature, (*cyclo*-$AsP_2$)CrCp(CO)$_2$, was also formed concomitantly with its *cyclo*-$P_3$ analogue.[46] The pair was synthesized by treating the tetrahedral complex [CrCp(CO)$_2$]$_2$($\mu$-$\eta^2$-$P_2$) with one equivalent of $AsCl_3$, and the *cyclo*-$AsP_2$ complex ($\delta = -242$ ppm) appeared 43 ppm downfield from the *cyclo*-$P_3$ complex ($\delta = -285$ ppm) in the $^{31}P$ NMR spectrum. Crystals of (*cyclo*-$AsP_2$)CrCp(CO)$_2$ were obtained in 10% yield *via* fractional crystallization of the reaction mixture. The formation of (*cyclo*-$AsP_2$)Mo(N[$^i$Pr]Ar)$_3$, **7**, can be explained by a suprafacial [2 + 2] cycloaddition reaction between As≡P and P≡Mo(N[$^i$Pr]Ar)$_3$, followed by rapid intramolecular isomerization to the molybdenum *cyclo*-$AsP_2$ complex.[16] The mechanism for As/P exchange to form (*cyclo*-$P_3$)Mo(N[$^i$Pr]Ar)$_3$ has not been elucidated, and presumably involves a bimolecular process.

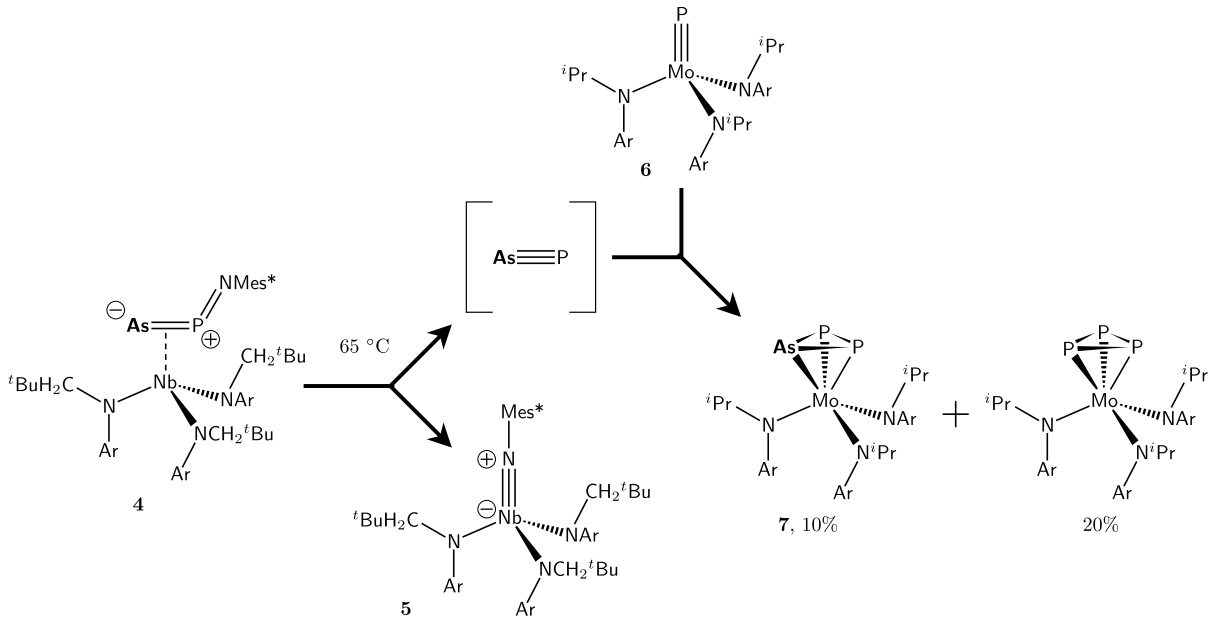


Figure 5: Thermolysis of the As=P=NMes* complex **4** results in fragmentation to the niobium imido **5** and the putative As≡P molecule. The latter fragment is absorbed by molybdenum terminal phosphide **6** to yield the new *cyclo*-$AsP_2$ complex **7**.

## Synthesis of the $(AsP)W(CO)_5$ Synthon

In an effort to stabilize AsP in solution after its extrusion from the $Nb(N[Np]Ar)_3$ platform, we investigated the possibility of its generation as a tungsten pentacarbonyl complex. We have observed previously that coordination of the $W(CO)_5$ fragment to the terminal P atom of ($\eta^2$-PPNMes*)$Nb(N[Np]Ar)_3$ results in room temperature fragmentation of the complex to the $(P_2)W(CO)_5$ molecule and the niobium imido **5**.[15] Binding of $W(CO)_5$ sufficiently stabilizes the $P_2$ molecule to extend its lifetime in solution, but does not shut down the triple bond reactivity of the diphosphorus moiety. Higher yields of trapping products are generally observed for $(P_2)W(CO)_5$ than for the unsupported $P_2$ molecule.[15–17]

Treatment of [Na(THF)][As≡$Nb(N[Np]Ar)_3$], [Na(THF)][**3**], with a solution of $W(CO)_5$(THF) resulted in conversion to the $W(CO)_5$-capped arsenide salt [Na(THF)][$(OC)_5$WAs≡Nb-$(N[Np]Ar)_3$], [Na(THF)][**3**-$W(CO)_5$], which can be isolated as a red solid in 55% yield. Addition of one equivalent of ClP=NMes* to a solution of [Na(THF)][**3**-$W(CO)_5$] in thawing $Et_2O$ resulted in formation

of $(OC)_5W(\eta^2$-AsPNMes*)Nb(N[Np]Ar)$_3$, **4**-W(CO)$_5$, *via* an NaCl elimination reaction. Complex **4**-W(CO)$_5$ is thermally unstable and readily fragments to (Mes*N)Nb(N[Np]Ar)$_3$, **5**, and the (AsP)W(CO)$_5$ unit, even at temperatures below 0 °C. At 10 °C in toluene-$d_8$ solution, **4**-W(CO)$_5$ is observed to decay following clean first-order kinetics with a rate constant $k = 5.5(3) \times 10^{-4}$ s$^{-1}$. The free (AsP)W(CO)$_5$ molecule was not directly observed by $^{31}$P NMR spectroscopy.

## Trapping of the (AsP)W(CO)$_5$ Molecule

Having already obtained a measure of success in trapping unsupported AsP with P≡Mo(N[$^i$Pr]Ar)$_3$, **6**, we turned our attention to trapping (AsP)W(CO)$_5$ with the same molybdenum complex. Addition of one equivalent of **6** to a thawing $Et_2O$ solution of **4**-W(CO)$_5$ yielded a mixture of (Mes*N)Nb(N[Np]Ar)$_3$, **5**, and $(OC)_5W$(*cyclo*-$AsP_2$)Mo(N[$^i$Pr]Ar)$_3$, **7**-W(CO)$_5$ (Figure 6). Although **7**-W(CO)$_5$ was observed to form in 70% yield by $^1$H NMR spectroscopy, the required separation from **5** resulted in a much lower isolated yield for the red, crystalline solid of 31%. At 20 °C in benzene-$d_6$, **7**-W(CO)$_5$ appears as a broad resonance at $\delta = -169$ ppm in the $^{31}$P NMR spectrum, presumably resulting from circumambulation of the W(CO)$_5$ fragment about the *cyclo*-$AsP_2$ ring. For comparison, the related *cyclo*-$P_3$ complex, $(OC)_5W$(*cyclo*-$P_3$)Mo(N[$^i$Pr]Ar)$_3$, formed by the trapping of $(P_2)W(CO)_5$ by **6**, resonates at $\delta = -212$ ppm (20 °C, benzene-$d_6$).[16] A small amount of (*cyclo*-$AsP_2$)Mo(N[$^i$Pr]Ar)$_3$ missing the W(CO)$_5$ cap ($\delta = -137$ ppm) is always observable in the baseline of $^{31}$P NMR spectra of **7**-W(CO)$_5$, despite the established purity of the sample by elemental analysis.

A solution of **7**-W(CO)$_5$ in toluene-$d_8$ was analyzed by variable-temperature $^{31}$P NMR spectroscopy. At 50 °C, the resonance at $\delta = -169$ ppm sharpened significantly, revealing other small peaks in the baseline at $\delta = -185$ and $\delta = -212$ ppm, which have been assigned as (*cyclo*-$P_3$)Mo(N[$^i$Pr]Ar)$_3$ and $(OC)_5W$(*cyclo*-$P_3$)Mo(N[$^i$Pr]Ar)$_3$, respectively. This demonstrated that As/P exchange may also be occurring in the (AsP)W(CO)$_5$ trapping reaction with **6**, but to a much lesser extent than with the unsupported AsP molecule. Locking out of the different phosphorus environments in **7**-W(CO)$_5$ did not occur until the temperature of the sample was lowered to −80

°C. At this temperature, a complex pattern of sharp doublets ($J_{PP}$ = ca. 300 Hz) emerged.[34] At low temperature, a propeller-like $C_3$ conformation of the anilide ligands is locked out as well as the migration of the $W(CO)_5$ about the $AsP_2$ ring. This makes both the $W(CO)_5AsP_2$ fragment and niobium anilide fragment of the complex chiral. With two inequivalent phosphorus nuclei, locking out the $W(CO)_5$ fragment on each of As, P1, and P2, gives rise to six expected $^{31}P$ NMR resonances. The additional resonances observed are most likely a consequence of the small amounts of (*cyclo*-$AsP_2$)Mo(N[$^i$Pr]Ar)$_3$, (*cyclo*-$P_3$)Mo(N[$^i$Pr]Ar)$_3$, and $(OC)_5$W(*cyclo*-$P_3$)Mo(N[$^i$Pr]Ar)$_3$ also present in solution.

The solid state structure of **7**-$W(CO)_5$ exhibits the expected geometry, with the *cyclo*-$AsP_2$ ring $\eta^3$-coordinated to the molybdenum trisanilide platform (Figure 7). Of note, the $W(CO)_5$ fragment is $\eta^1$-coordinated to phosphorus and not to the arsenic atom to which it was bound in [**3**-$W(CO)_5$]$^-$. This is not surprising considering the relative nucleophilicities of phosphorus and arsenic, and the established ability of the $W(CO)_5$ fragment to circumambulate the *cyclo*-$AsP_2$ ring in solution. Atoms P1 and As1 are site disordered in the crystal structure of **7**-$W(CO)_5$, with the major contributor (57%) being shown in Figure 7. As/P site disorder is also observed in the solid state structure of the *cyclo*-$AsP_2$ complex (*cyclo*-$AsP_2$)$CrCp(CO)_2$; however, in this case the arsenic atom is disordered over all three positions in the ring.[46] The bonds about the *cyclo*-$AsP_2$ ring in the solid state structure of **7**-$W(CO)_5$ are all essentially equal in length ($r_{As—P1}$ = 2.284(9) Å, $r_{As—P2}$ = 2.227(3) Å, $r_{P1—P2}$ = 2.223(12) Å), which is likely a consequence of the site disorder and not a true reflection of the bonding situation in the complex. A geometry optimization performed on the model complex $(OC)_5$W(*cyclo*-$AsP_2$)Mo(N[Me]Ph)$_3$ predicted two different As—P bond lengths in this structure ($r_{As—P}$ = 2.328 Å, $r_{As—P}$ = 2.244 Å), with the shorter distance involving the phosphorus atom bound to $W(CO)_5$ (Table 1).

Trapping of the $(AsP)W(CO)_5$ molecule can also be achieved by addition of 10 equivalents of either 1,3-cyclohexadiene ($C_6H_8$) or 2,3-dimethyl-1,3-butadiene ($C_6H_{10}$) to a thawing $Et_2O$ solution of **4**-$W(CO)_5$ (Figure 6) and allowing the reaction mixture to warm slowly to room temperature. Following separation from (Mes*N)Nb(N[Np]Ar)$_3$ (**5**), the $W(CO)_5$-complexed double

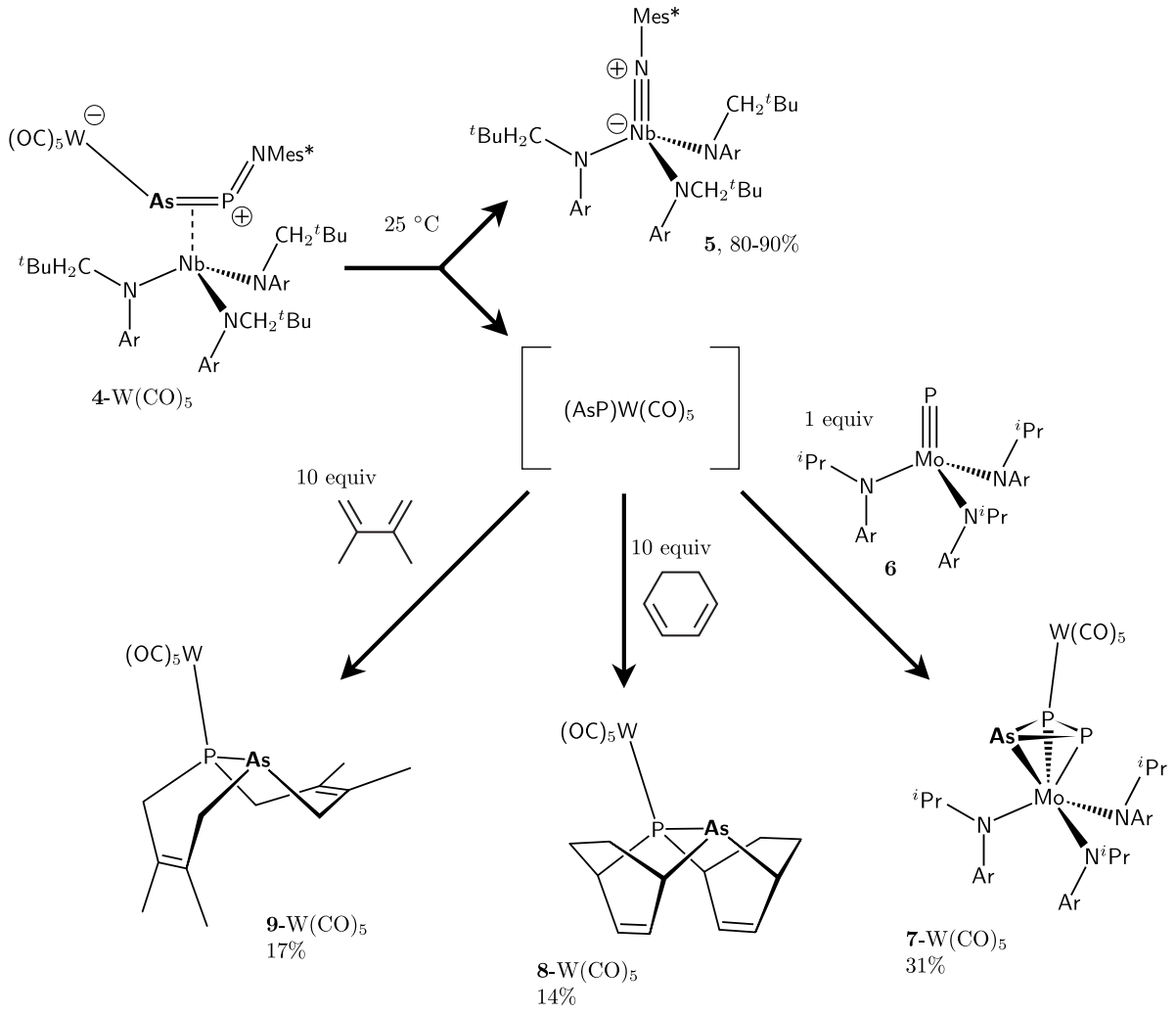


Figure 6: Thermal fragmentation of complex **4**-W(CO)$_5$ in the presence of various trapping agents. Yields shown for the ostensible products of (AsP)W(CO)$_5$ trapping are isolated yields of pure material after separation from co-product imido **5**.

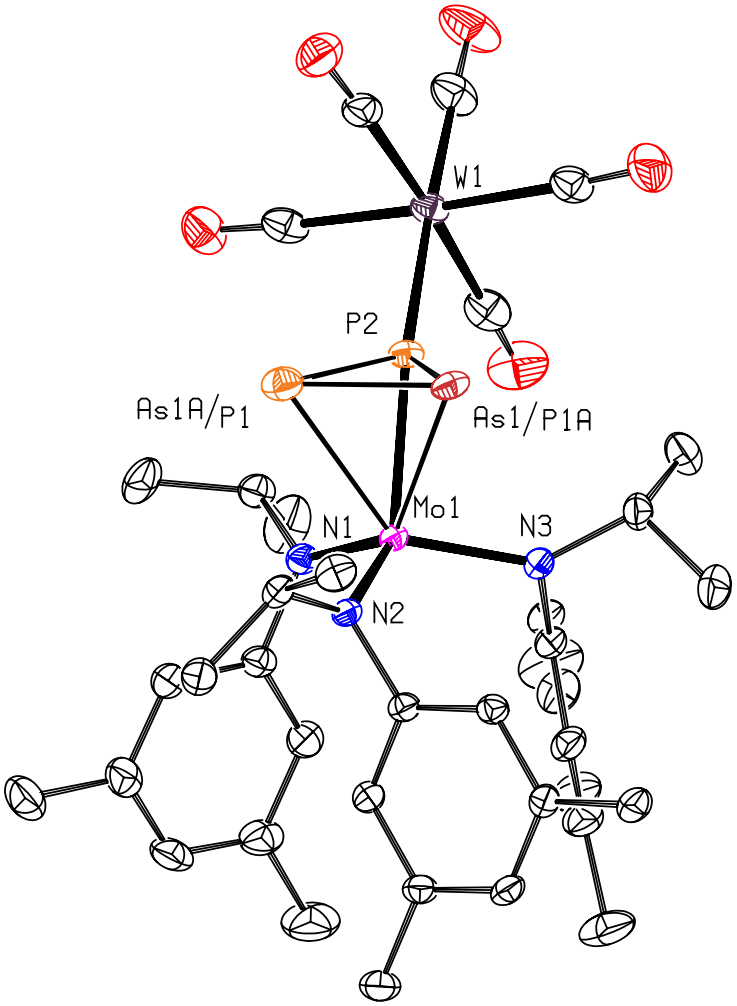


Figure 7: Molecular structure of complex **7**-$W(CO)_5$ shown with 50% probability thermal ellipsoids. The atoms As1 and P1 are site disordered in the solid state structure with the major contributor (57%) shown. Selected interatomic distances (Å) and angles (°): As1–P1, 2.284(9); As1–P2, 2.227(3); P1–P2, 2.223(12); P2–W1, 2.5463(7); Mo1–As1, 2.611(2); Mo1–P1, 2.636(12); Mo1–P2, 2.4759(7); P2–P1–As1, 59.2(3); P1–P2–As1, 61.8(3); P1–P2–W1, 130.6(3), P2–As1–P1, 59.0(3).

Diels-Alder adducts of AsP, $(OC)_5W(AsP)(C_6H_8)_2$ (**8**-$W(CO)_5$) and $(OC)_5W(AsP)(C_6H_{10})_2$ (**9**-$W(CO)_5$) were isolated as white crystalline solids in 14% and 17% yields, respectively. Monitoring formation of **8**-$W(CO)_5$ and **9**-$W(CO)_5$ in solution by $^{31}P$ NMR spectroscopy ($PPh_3$ as internal standard) gave much higher yields of 46% and 52%, indicating that $(AsP)W(CO)_5$ is trapped much more efficiently by organic dienes than AsP. The formulations of **8**-$W(CO)_5$ and **9**-$W(CO)_5$ were confirmed by high-resolution electron impact mass spectrometry; the molecular ions of both species were located and matched the predicted isotope patterns for $(OC)_5W(AsP)(C_6H_8)_2$ and $(OC)_5W(AsP)(C_6H_{10})_2$. Of note, the $(AsP)W(CO)_5$ radical cation was also observed in the mass spectrum of both **8**-$W(CO)_5$ and **9**-$W(CO)_5$.

The $^{31}P$ NMR spectra of compounds **8**-$W(CO)_5$ ($\delta = -23$ ppm, $J_{WP} = 219$ Hz) and **9**-$W(CO)_5$ ($\delta = -12$ ppm, $J_{WP} = 225$ Hz) exhibit singlets flanked by $^{183}W$ satellites, indicating that migration of the $W(CO)_5$ fragment from arsenic to phoshorus has occurred during the course of the reaction. Indeed, the solid-state structures of the double Diels-Alder adducts **8**-$W(CO)_5$ (Figure 8) and **9**-$W(CO)_5$ (Figure 9) confirm that $W(CO)_5$ is bound to phosphorus in the final products. The $(P_2)W(CO)_5$ and $(As_2)W(CO)_5$ molecules have been the subject of a theoretical study concluding that, in contrast to $N_2$, the $P_2$ and $As_2$ ligands preferentially bind side-on to the W center.[47] If the same is assumed to be true for $(AsP)W(CO)_5$, it is easy to envision migration of the $W(CO)_5$ fragment along the As—P bond to the more nucleophilic phoshorus atom during the trapping reactions.

Compounds **8**-$W(CO)_5$ and **9**-$W(CO)_5$ are isostructural to the related $(P_2)W(CO)_5$ double Diels-Alder adducts of 1,3-cyclohexadiene and 2,3-dimethyl-1,3-butadiene,[15] with the exception of the slightly longer As—P bond distances (**8**-$W(CO)_5$, $r_{As—P} = 2.3010(6)$ Å; **9**-$W(CO)_5$, $r_{As—P} = 2.3195(11)$ Å). The double 1,3-cyclohexadiene adduct, **8**-$W(CO)_5$, exhibits a tetracyclic structure with a cofacial pair of C=C $\pi$ bonds, while the double 2,3-dimethyl-1,3-butadiene adduct, **9**-$W(CO)_5$, exhibits a more open bicyclic framework. The structure of **8**-$W(CO)_5$ was geometry optimized using DFT calculations (Table 1), giving a calculated $r_{As—P} = 2.297$ Å, which agrees well with the As—P bond lengths observed in the solid state structures of **8**-$W(CO)_5$ and **9**-$W(CO)_5$ and

the predicted As—P bond length from single bond covalent radii (2.32 Å).[28]

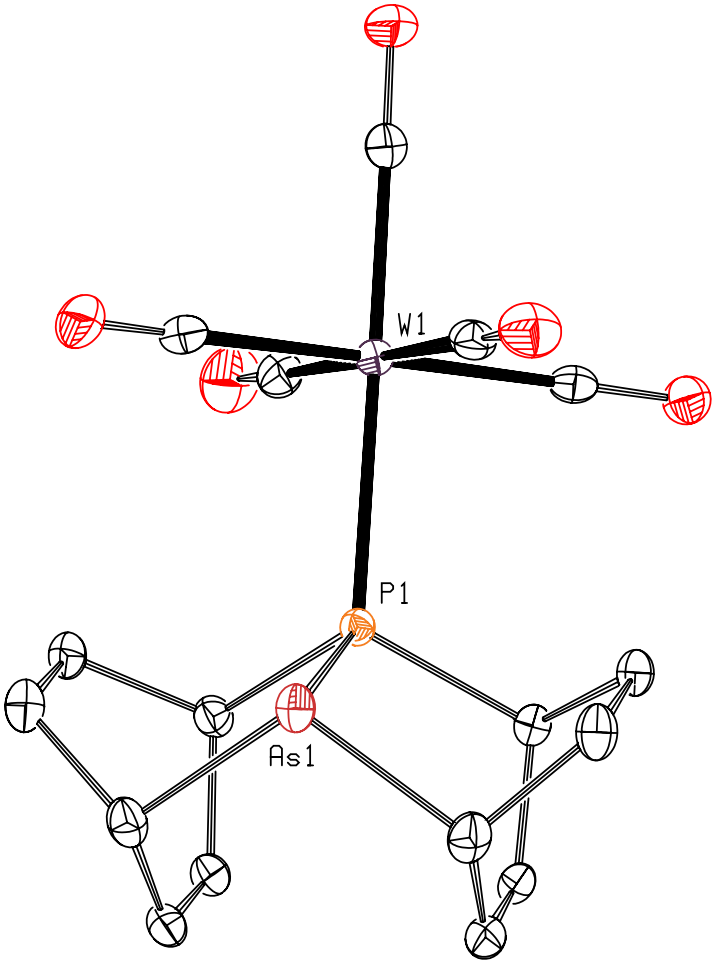


Figure 8: Molecular structure of complex **8**-$W(CO)_5$ shown with 50% probability thermal ellipsoids. Selected interatomic distances (Å) and angles (°): As1–P1, 2.3010(6); P1–W1, 2.5405(5); As1–P1–W1, 116.22(2).

## Conclusions

In conclusion, we have used the niobium-mediated acivation chemistry of $As_4$ to access the unsaturated intermediate $(AsP)W(CO)_5$ in solution. Despite being bound by tungsten pentacarbonyl, the AsP moiety retains its triple bond reactivity, as witnessed by its ability to react with two equivalents of organic diene in Diels-Alder reactions. The $(AsP)W(CO)_5$ molecule also reacts in a one-to-one fashion with $P{\equiv}Mo(N[^{i}Pr]Ar)_3$ (**6**) to generate the new *cyclo*-$AsP_2$ molybdenum com-

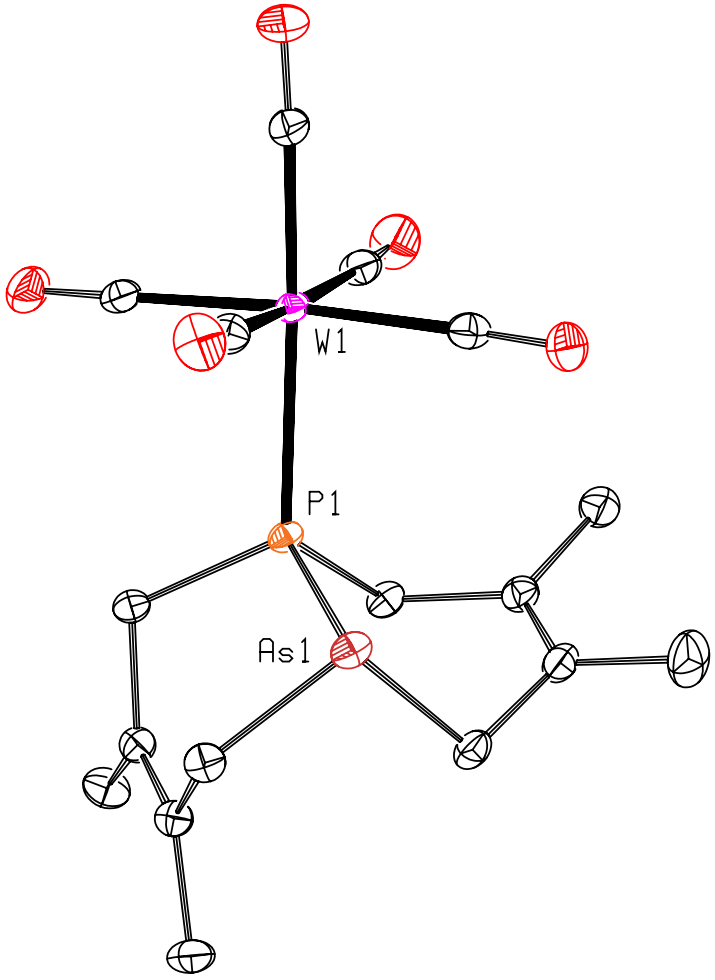


Figure 9: Molecular structure of complex **9**-$W(CO)_5$ shown with 50% probability thermal ellipsoids. Selected interatomic distances (Å) and angles (°): As1–P1, 2.3195(11); P1–W1, 2.5191(11); As1–P1–W1, 112.64(4).

plex, $(OC)_5W(cyclo\text{-}AsP_2)Mo(N[^iPr]Ar)_3$ (**7**-$W(CO)_5$), which has been structurally characterized. In addition to accessing triple-bond reactivity of the proposed $(AsP)W(CO)_5$ intermediate, this work has yielded a simple mononuclear niobium terminal arsenide anion, $[As{\equiv}Nb(N[Np]Ar)_3]^-$ (**3**), which contains a Nb—As triple bond. The anionic charge in **3** facilitates functionalization of the terminal arsenide unit, allowing for the synthesis of the new As=P=NMes* ligand atop the niobium trisanilide framework. Thermolysis of the arsaphosphaazide complex ($\eta^2$-AsPNMes*)Nb-$(N[Np]Ar)_3$ (**4**) results in near quantitative conversion to the niobium imido $(Mes*N)Nb(N[Np]Ar)_3$ (**5**), with concomitant loss of the AsP diatomic unit. Trapping reactions involving the As≡P molecule gave very low yields or complex mixtures of products, suggesting that this molecule is less tractable in terms of trapping or transfer than was the case for P≡P when accessed using similar methodology. The synthetic explorations reported herein represent a dual effort to discover triple-bond reactivity for low-coordinate arsenic while defining methods for arsenic incorporation that stem from the element itself.

# Experimental

## General Procedures

All manipulations were performed in a Vacuum Atmospheres model MO-40M glovebox under an atmosphere of purified $N_2$. Solvents were obtained anhydrous and oxygen-free from a Contour Glass Solvent Purification System. Deuterated solvents for NMR spectroscopy were purchased from Cambridge Isotope Labs. Benzene-$d_6$ and toluene-$d_8$ were degassed and stored over molecular sieves for at least 2 days prior to use. THF-$d_8$ was distilled from sodium/benzophenone and stored over molecular sieves at −35 °C. Celite 435 (EM Science), 4 Å molecular sieves (Aldrich), and alumina (EM Science) were dried by heating at 200 °C under dynamic vacuum for at least 24 hours prior to use. 1,3-Cyclohexadiene and 2,3-dimethyl-1,3-butadiene were purchased from Aldrich, distilled from $NaBH_4$, and stored over molecular sieves at −35 °C prior to use. Tungsten hexacarbonyl was purchased from Strem and used without further purification. The com-

pounds HNb($\eta^2$-$^t$BuHC=NAr)(N[Np]Ar)$_2$ (**1**),[11] Mes*NPCl,[14] and P≡Mo(N[$^i$Pr]Ar)$_3$ (**6**)[44] were prepared according to literature procedures. All glassware was oven-dried at temperatures greater than 170 °C prior to use. NMR spectra were obtained on Bruker Avance 400, Varian Mercury 300, or Varian Inova 500 spectrometers. $^1$H NMR spectra were referenced to residual solvent resonances ($C_6D_5H$, 7.16 ppm, $C_4D_7HO$, 3.58 ppm, $C_7D_7H$, 2.09 ppm); $^{13}$C NMR spectra were referenced to $C_6D_6$ (128.39 ppm) and $C_4D_8O$ (67.57 ppm); and $^{31}$P NMR spectra were referenced externally to 85% $H_3PO_4$ (0 ppm). Elemental analyses were performed by Midwest Microlab, LLC, Indianapolis, Indiana.

## $As_4$ Generation and Trapping

Yellow arsenic ($As_4$) is generated by subliming grey arsenic in the apparatus shown in Supporting Information Figure S1. In a typical run, approximately 5 g of grey arsenic is loaded into the middle of the inner horizontal steel tube and heated to a temperature of 515-550 °C for a period of three hours. A stream of argon gas (flow rate: 1 L/min) carries the $As_4$ vapors into the T-joint, where they meet another stream of room temperature argon (flow rate: 1 L/min). The argon/$As_4$ mixture is bubbled through a flask containing 500 mL of chilled toluene (−30 °C, bath: 50/50 water/ethylene glycol + liquid $N_2$), where the $As_4$ vapors condense in solution. The argon stream leaves the flask and passes through a series of three bleach-filled bubblers to scrub out any escaping arsenic vapors. The entire procedure is performed in the dark to prevent conversion of $As_4$ to grey arsenic. The saturated solution of $As_4$ in toluene is then used in the subsequent synthesis of **2**, without the isolation of solid $As_4$. It is apparent that not all the $As_4$ remains in solution, as gram quantities of grey arsenic are always observed in the flask after sublimation.

## Synthesis of ($\mu_2$:$\eta^2$,$\eta^2$-$As_2$)[Nb(N[Np]Ar)$_3$]$_2$, 2

In the dark, HNb($\eta^2$-$^t$BuHC=NAr)(N[Np]Ar)$_2$ (**1**, 1.81 g, 2.73 mmol), was added under an argon stream to a cold solution of $As_4$ in toluene (−30 °C; generated as described above) by means of a solid addition funnel. The reaction mixture was kept in the dark, allowed to warm to room

temperature, and stirred for 16 h, during which time the color of the solution changed from orange to dark green. The product of the reaction is not light-sensitive, and no further precautions to exclude light were taken during the subsequent workup. The toluene was removed under vacuum, and the resulting green-black residue was taken up in *n*-hexane (400 mL) and filtered through Celite to remove solid arsenic and other insoluble materials. The dark green solution was then evaporated to dryness and the solids obtained thereby were slurried in *n*-pentane (60 mL). The pentane slurry was placed in the freezer for 16 h at −35 °C to induce further precipitation. A bright green powder was isolated by filtration and washed with cold *n*-pentane. The filtrate was concentrated, placed back in the freezer and a second crop of the green powder was isolated. Total yield: 1.04 g, 0.704 mmol, 52%. Elem. Anal. Calcd. for $C_{78}H_{120}N_6As_2Nb_2$: C, 63.41; H, 8.19; N, 5.69. Found: C, 62.61; H, 8.07; N, 5.72. $^1$H NMR (benzene-$d_6$, 20 °C, 500 MHz): $\delta$ = 6.95 (bs, 12H, *o*-Ar), 6.58 (s, 6H, *p*-Ar), 4.26 (bs, 12H, N-C$H_2$), 2.23 (s, 36H, Ar-C$H_3$), 0.99 (s, 54H, C(C$H_3$)$_3$) ppm. $^{13}$C{$^1$H} NMR (benzene-$d_6$, 20 °C, 125.8 MHz): $\delta$ = 154.2 (bs, aryl *ipso*), 138.2 (s, *m*-Ar), 126.6 (s, *p*-Ar), 124.2 (bs, *o*-Ar), 73.5 (bs, N-*C*H$_2$), 37.3 (bs, *C*(CH$_3$)$_3$), 30.7 (s, C(*C*H$_3$)$_3$), 22.1 (s, Ar-*C*H$_3$) ppm. FTIR (KBr windows, thin film): 2945(s), 1585(s), 1473(s), 1394(m), 1363(m), 1286(m), 1154(m), 1064(m), 999(s), 842(s), 683(s) cm$^{-1}$.

## Synthesis of [Na(THF)][As≡Nb(N[Np]Ar)$_3$], [Na(THF)][3]

Freshly prepared 1% sodium amalgam (Na: 0.25 g, 11 mmol, 15 equiv/Nb) was added to a dark green THF (30 mL) solution of ($\mu_2$:$\eta^2$,$\eta^2$-As$_2$)[Nb(N[Np]Ar)$_3$]$_2$ (**2**, 1.09 g, 0.740 mmol). The mixture was stirred vigorously for 2 h, during which time the color gradually changed from green to bright red. The supernatant solution was decanted from the amalgam and evaporated to dryness, leaving behind a red residue. The red residue was extracted with 50 mL of *n*-pentane and filtered through Celite. The filtrate was concentrated to a volume of 3 mL and placed in the freezer for 16 h at −35 °C, during which time a bright orange microcrystalline precipitate deposited. The orange precipitate was isolated by filtration and washed with 1 mL of cold *n*-pentane. The filtrate was concentrated, placed back in the freezer and a second crop of orange powder was isolated.

Total yield: 0.836 g, 1.00 mmol, 68%. Crystals suitable for X-ray diffraction were grown over a period of 16 h from a concentrated pentane solution kept at −35 °C. Elem. Anal. Calcd. for $C_{43}H_{68}N_3ONaAsNb$: C, 61.94; H, 8.22; N, 5.04. Found: C, 61.98; H, 8.33; N, 4.96. $^1$H NMR (benzene-$d_6$, 20 °C, 400 MHz): $\delta$ = 6.99 (s, 6H, *o*-Ar), 6.48 (s, 3H, *p*-Ar), 4.37 (s, 6H, N-C$H_2$), 3.67 (m, 4H, THF), 2.24 (s, 18H, Ar-C$H_3$), 1.56 (m, 4H, THF), 1.13 (s, 27H, C(C$H_3$)$_3$) ppm. $^{13}$C{$^1$H} NMR (benzene-$d_6$, 20 °C, 100.6 MHz): $\delta$ = 158.8 (s, aryl *ipso*), 138.7 (s, *m*-Ar), 123.3 (s, *p*-Ar), 122.0 (s, *o*-Ar), 75.2 (bs, N-*C*H$_2$), 68.8 (s, THF), 36.6 (s, *C*(CH$_3$)$_3$), 30.2 (s, C(*C*H$_3$)$_3$), 26.1 (s, THF), 22.2 (s, Ar-*C*H$_3$) ppm. FTIR (KBr windows, nujol mull): 1585(s), 1573(m), 1363(m), 1292(m), 1152(m), 994(m), 840(m), 680(s), 675(s) cm$^{-1}$.

## Synthesis of [Na(12-crown-4)$_2$][As≡Nb(N[Np]Ar)$_3$], [(Na(12-c-4)$_2$][3]

A solution of 0.084 g of 12-crown-4 (0.48 mmol, 2.7 equivalents) in 3 mL of *n*-pentane was added dropwise with stirring to a solution of [Na(THF)][As≡Nb(N[Np]Ar)$_3$] ([Na(THF)][**3**], 0.150 g, 0.180 mmol) in *n*-pentane (3 mL). The red color of the solution faded and a yellow precipitate formed. The reaction mixture was allowed to stir for 30 min and then placed in the freezer for 16 h at −35 °C to induce further precipitation. The yellow powder was isolated by filtration and washed with cold *n*-pentane (3 mL). Total yield: 0.153 g, 0.137 mmol, 76%. Crystals suitable for X-ray diffraction were grown by adding 3 mL of *n*-pentane to the yellow powder, followed by the dropwise addition of $Et_2O$ until all the material dissolved. The *n*-pentane/$Et_2O$ mixture was placed in the freezer for one week at −35 °C, during which time crystals deposited. Elem. Anal. Calcd. for $C_{55}H_{92}N_3O_8NaAsNb$: C, 59.29; H, 8.32; N, 3.77. Found: C, 58.84; H, 8.10; N, 3.80. $^1$H NMR (benzene-$d_6$, 20 °C, 500 MHz): $\delta$ = 7.02 (s, 6H, *o*-Ar), 6.42 (s, 3H, *p*-Ar), 4.98 (bs, 6H, N-C$H_2$), 3.20 (s, 24H, crown), 2.25 (s, 18H, Ar-C$H_3$), 1.46 (s, 27H, C(C$H_3$)$_3$) ppm. $^{13}$C{$^1$H} NMR (benzene-$d_6$, 20 °C, 125.8 MHz): $\delta$ = 157.6 (s, aryl *ipso*), 137.4 (s, *m*-Ar), 121.3 (s, *p*-Ar), 120.9 (s, *o*-Ar), 76.9 (bs, N-*C*H$_2$), 66.0 (s, crown), 36.9 (s, *C*(CH$_3$)$_3$), 31.0 (s, C(*C*H$_3$)$_3$), 22.4 (s, Ar-*C*H$_3$) ppm. FTIR (KBr windows, nujol mull): 1582(m), 1365(m), 1289(m), 1135(s), 1095(s), 1021(s), 916(m), 674(m) cm$^{-1}$.

## Synthesis of [Na][$(OC)_5$WAs≡Nb(N[Np]Ar)$_3$], [Na][3-W(CO)$_5$]

A 0.015 M yellow solution of W(CO)$_5$(THF) was prepared by irradiating a solution of W(CO)$_6$ (0.650 g, 1.85 mmol) in 50 mL of THF in a Rayonet photoreactor equipped with six RPR-4190 (emission maximum at 419 nm) and ten RPR-2540 (emission maximum at 254 nm) lamps for 24 h, with periodic degassing to remove CO. To this solution (42 mL, 0.630 mmol of W(CO)$_5$(THF)) was added 0.525 g of [Na(THF)][As≡Nb(N[Np]Ar)$_3$] ([Na(THF)][**3**], 0.630 mmol), and the dark red reaction mixture was stirred for 2 h and then pumped down to dryness to yield a dark red residue. The residue was taken up in 50 mL of pentane and filtered through Celite to remove excess W(CO)$_6$. The red filtrate was pumped down to dryness and a $^1$H NMR of the crude material showed quantitative conversion of [Na(THF)][**3**] to the W(CO)$_5$-capped analogue [Na(THF)][**3**-W(CO)$_5$]. To obtain analytically pure material, the red residue was taken up in 8 mL of $Et_2O$ and placed in the freezer for 16 h at −35 °C. During this time, white crystals of W(CO)$_6$ deposited. The red supernatant solution was filtered, concentrated to a volume of 4 mL, and placed back in the freezer. More W(CO)$_6$ was removed by filtration and the red supernatant solution was pumped down to dryness to yield an oily red solid. The red solid was slurried in 2 mL of *n*-pentane and placed in the freezer for 16 h at −35 °C. A fine red powder precipitated and was isolated by filtration and washed with a further 2 mL of cold *n*-pentane. Total yield: 0.373 g, 0.344 mmol, 55%. The red powder was further purified by heating for 2 h at 70 °C in a sublimation apparatus under dynamic vacuum. A few additional mg of W(CO)$_6$ contaminant was collected on the cold finger. Elem. Anal. Calcd. for $C_{44}H_{60}N_3O_5NaAsNbW$: C, 48.68; H, 5.57; N, 3.87. Found: C, 48.88; H, 5.66; N, 3.25. $^1$H NMR (benzene-$d_6$, 20 °C, 500 MHz): $\delta$ = 6.98 (s, 6H, *o*-Ar), 6.46 (s, 3H, *p*-Ar), 4.09 (s, 6H, N-C$H_2$), 2.18 (s, 18H, Ar-C$H_3$), 1.10 (s, 27H, C(C$H_3$)$_3$) ppm. $^{13}$C{$^1$H} NMR (benzene-$d_6$, 20 °C, 125.8 MHz): $\delta$ = 208.3 (s, *trans* CO), 202.3 (s, *cis* CO, $J_{CW}$ = 125 Hz), 157.7 (s, aryl *ipso*), 139.2 (s, *m*-Ar), 124.3 (s, *p*-Ar), 122.0 (s, *o*-Ar), 73.8 (bs, N-$CH_2$), 36.4 (s, $C(CH_3)_3$), 30.0 (s, C($CH_3$)$_3$), 21.9 (s, Ar-$CH_3$) ppm. FTIR (KBr windows, nujol mull): 2349(m), 2052(s), 1968(s), 1928(vs), 1809(vs), 1584(s), 1365(s), 1155(s), 995(s), 844(s), 687(s), 581(s) cm$^{-1}$.

## Synthesis of ($\eta^2$-AsPNMes*)Nb(N[Np]Ar)$_3$, 4

To a stirring, thawing $Et_2O$ solution (30 mL) of [Na(THF)][As≡Nb(N[Np]Ar)$_3$] ([Na(THF)][**3**], 0.496 g, 0.595 mmol) was added dropwise a thawing solution of Mes*NPCl (0.212 g, 0.651 mmol, 1.1 eq) in $Et_2O$ (3 mL). The dark red reaction mixture was allowed to stir while warming to room temperature over 30 min and was then pumped down to dryness. The remaining red residue was taken up in 25 mL of *n*-pentane and filtered through Celite to remove NaCl. A $^{31}P\{^1H\}$ NMR spectrum of the filtrate showed quantitative conversion to the arsaphosphaazide complex ($\eta^2$-AsPNMes*)Nb(N[Np]Ar)$_3$, **4**. The *n*-pentane filtrate was concentrated to a volume of 2 mL and placed in the freezer for 16 h at −35 °C, during which time a dark red-orange powder precipitated. The powder was collected by filtration and washed with an additional 1 mL of cold *n*-pentane. Total yield: 0.3127 g, 0.304 mmol, 51%. Crystals suitable for X-ray diffraction were obtained by dissolving the powder in a 50/50 $Et_2O$/$(Me_3Si)_2O$ mixture and placing the resulting solution in the freezer for 16 h at −35 °C. Elem. Anal. Calcd. for $C_{57}H_{89}N_4PAsNb$: C, 66.52; H, 8.72; N, 5.44. Found: C, 66.49; H, 8.68; N, 5.43. $^1H$ NMR (benzene-$d_6$, 20 °C, 500 MHz): $\delta$ = 7.76 (s, 2H, *m*-Mes*), 6.63 (s, 6H, *o*-Ar), 6.58 (s, 3H, *p*-Ar), 4.11 (s, 6H, N-C$H_2$), 2.12 (s, 18H, Ar-C$H_3$), 1.93 (s, 18H, *o*-C(C$H_3$)$_3$ Mes*), 1.48 (s, 9H, *p*-C(C$H_3$)$_3$ Mes*), 0.82 (s, 27H, $CH_2$-C(C$H_3$)$_3$) ppm. $^{13}C\{^1H\}$ NMR (benzene-$d_6$, 20 °C, 125.8 MHz): $\delta$ = 152.2 (s, aryl *ipso*), 151.3 (d, $J_{CP}$ = 36 Hz, Mes* *ipso*), 142.8 (d, $J_{CP}$ = 5 Hz, *m*-Mes*), 139.4 (d, $J_{CP}$ = 12 Hz, *o*-Mes*), 138.6 (s, *m*-Ar), 127.6 (s, *p*-Ar), 124.3 (s, *o*-Ar), 122.7 (d, $J_{CP}$ = 5 Hz, *p*-Mes*), 73.1 (d, $J_{CP}$ = 7 Hz, N-*C*$H_2$), 37.3 (d, $J_{CP}$ = 2 Hz, *o*-*C*$(CH_3)_3$ Mes*), 37.1 (s, $CH_2$-*C*$(CH_3)_3$), 35.2 (d, $J_{CP}$ = 1 Hz, *p*-*C*$(CH_3)_3$ Mes*), 33.6 (s, *o*-C(*C*$H_3$)$_3$ Mes*), 32.5 (s, *p*-C(*C*$H_3$)$_3$ Mes*), 30.2 (s, $CH_2$-C(*C*$H_3$)$_3$), 21.9 (s, Ar-*C*$H_3$) ppm. $^{31}P\{^1H\}$ NMR (benzene-$d_6$, 20 °C, 121.5 MHz): $\delta$ = 349 (s) ppm. FTIR (KBr windows, nujol mull): 1602(m), 1587(s), 1416(s), 1365(s), 1311(s), 1293(s), 996(m), 848(m), 692(m), 684(m) $cm^{-1}$.

## Synthesis of $(OC)_5W(cyclo\text{-}AsP_2)Mo(N[^iPr]Ar)_3$, 7-$W(CO)_5$

To a thawing solution of [Na(THF)][$(OC)_5$WAs≡Nb(N[Np]Ar)$_3$] ([Na(THF)][**3**-$W(CO)_5$], 0.300 g, 0.259 mmol) in $Et_2O$ (10 mL) was added a thawing $Et_2O$ (3 mL) solution of Mes*NPCl (0.085 g, 0.261 mmol, 1 eq) dropwise. After 30 s of stirring, a yellow $Et_2O$ (4 mL) solution of P≡Mo(N[$^i$Pr]Ar)$_3$ (**6**, 0.159 g, 0.259 mmol, 1 eq) was quickly added. There was no apparent color change to the dark red reaction mixture. After 3 h of stirring, the reaction mixture was pumped down to dryness, taken up in 30 mL of toluene and filtered through Celite to remove NaCl. The red filtrate was evaporated to dryness, leaving behind a red solid. The solid was slurried in 15 mL of *n*-hexane, and this mixture was placed in the freezer for 16 h at −35 °C. The red precipitate (0.285 g) was isolated by filtration and washed with 3 mL of *n*-hexane. Analysis by $^1$H NMR spectroscopy of this material revealed that it was composed of $(OC)_5W(cyclo\text{-}AsP_2)Mo(N[^iPr]Ar)_3$ (**7**-$W(CO)_5$, 68%) and (Mes*N)Nb(N[Np]Ar)$_3$ (**5**, 32%). The red solid was slurried in 5 mL of *n*-pentane and toluene was added dropwise until all the solids dissolved. The toluene/pentane mixture was placed in the freezer for 16 h at −35 °C, during which time dark red, block-shaped, X-ray quality crystals of **7**-$W(CO)_5$ grew. The red crystals were isolated by filtration and washed with 15 mL of cold *n*-pentane to remove small, yellow co-crystals of **5**. Total yield: 0.082 g, 0.079 mmol, 31%. Elem. Anal. Calcd. for $C_{38}H_{48}N_3O_5P_2AsMoW$: C, 43.74; H, 4.64; N, 4.03. Found: C, 43.91; H, 4.81; N, 4.02. $^1$H NMR (benzene-$d_6$, 20 °C, 500 MHz): $\delta$ = 6.68 (s, 3H, *p*-Ar), 6.27 (bs, 6H, *o*-Ar), 4.90 (bs, 3H, C*H*$(CH_3)_2$), 2.10 (s, 18H, Ar-C$H_3$), 0.91 (bs, 18H, CH(C$H_3)_2$) ppm. $^{13}$C{$^1$H} NMR (benzene-$d_6$, 20 °C, 125.8 MHz): $\delta$ = 197.9 (s, *cis* *C*O), 148.6 (bs, aryl *ipso*), 137.9 (s, *p*-Ar), 137.5 (s, *m*-Ar), 129.4 (s, *o*-Ar), 64.8 (bs, N-*C*H$(CH_3)_2$), 22.6 (bs, CH(*C*$H_3)_2$), 21.7 (s, Ar-*C*$H_3$) ppm. Note: The trans CO resonance was not located in the $^{13}$C{$^1$H} spectrum. $^{31}$P{$^1$H} NMR (benzene-$d_6$, 20 °C, 121.5 MHz): $\delta$ = −169 (bs) ppm. A small peak at $\delta$ = −139 ppm is also always observed and has been attributed to a small amount of $(cyclo\text{-}AsP_2)Mo(N[^iPr]Ar)_3$ (**7**) without the $W(CO)_5$ unit appended. FTIR (KBr windows, nujol mull): 2214(w), 2067(vs), 1980(vs), 1940(vs), 1599(s), 1583(m), 1357(s), 1152(s), 1107(s), 987(s), 933(s), 859(s), 687(vs), 593(vs), 573(vs) cm$^{-1}$.

## Synthesis of $(OC)_5W(AsP)(C_6H_8)_2$, 8-$W(CO)_5$

To a thawing solution of [Na(THF)][$(OC)_5$WAs≡Nb(N[Np]Ar)$_3$] ([Na(THF)][**3**-$W(CO)_5$], 0.200 g, 0.173 mmol) in $Et_2O$ (7 mL) was added dropwise a thawing $Et_2O$ (5 mL) solution of Mes*NPCl (0.057g, 0.175 mmol, 1 eq). After 30 s of stirring, 175 $\mu$L (1.78 mmol, 10.3 eq) of 1,3-cyclohexadiene was added *via* syringe. The dark red reaction mixture was stirred for 1 h and then pumped down to dryness, leaving behind a brown residue. The residue was extracted with 10 mL of toluene and filtered through Celite to remove NaCl. The red filtrate was evaporated to dryness and 5 mL of acetonitrile was added, resulting in precipitation of a yellow solid. The yellow solid was isolated by filtration, and characterized as the niobium imido complex, (Mes*N)Nb(N[Np]Ar)$_3$ (**5**, 0.1324 g, 0.143 mmol, 83% yield). The orange filtrate was evaporated to dryness and slurried in 2 mL of *n*-pentane. Diethyl ether was added dropwise to the slurry until all solids present dissolved and the mixture was placed in the freezer for 48 h at −35 °C. Colorless, X-ray quality crystals of **8**-$W(CO)_5$ were isolated by filtration and washed with 1 mL of cold *n*-pentane. Total yield: 0.015 g, 0.025 mmol, 14%. Note: Monitoring formation of **8**-$W(CO)_5$ *via* $^{31}$P NMR ($PPh_3$ as internal standard) gave an overall yield of 46%. $^1$H NMR (benzene-$d_6$, 20 °C, 500 MHz): $\delta$ = 5.18 (td, $J$ = 8 Hz and 4 Hz, 2H), 4.75 (td, $J$ = 8 Hz and 3.5 Hz, 2H), 2.55 (m, 4H), 1.70 (q, $J$ = 12 Hz, 2H), 1.23–1.17 (m, 2H), 1.13–1.06 (m, 2H), 0.93–0.78 (m, 2H) ppm. $^{13}$C{$^1$H} NMR (benzene-$d_6$, 20 °C, 125.8 MHz): $\delta$ = 199.2 (d, $J_{CP}$ = 24 Hz, *trans C*O), 197.9 (d, $J_{CP}$ = 6.5 Hz, $J_{CW}$ = 125 Hz, *cis C*O), 125.1 (d, $J_{CP}$ = 8 Hz), 124.5 (d, $J_{CP}$ = 10 Hz), 33.8 (d, $J_{CP}$ = 2 Hz), 32.2 (d, $J_{CP}$ = 4 Hz), 25.4 (d, $J_{CP}$ = 8 Hz), 23.0 (d, $J_{CP}$ = 5 Hz) ppm. $^{31}$P{$^1$H} NMR (benzene-$d_6$, 20 °C, 161.9 MHz): $\delta$ = −22 (s, $J_{WP}$ = 219 Hz) ppm. FTIR (KBr windows, thin film): 2171(m), 2064(s), 1971(m), 1918(vs), 1453(w), 1019(w), 725(w), 644(w), 616(w), 600(m), 573(s) cm$^{-1}$. HRMS-EI: Calcd. for $M^{+\cdot}$: 589.946. Found: 589.945. Also present: 509.882 ($W(CO)_5(AsP)(C_6H_8)^{+\cdot}$), 429.820 ($W(CO)_5(AsP)^{+\cdot}$), 401.825 ($W(CO)_4(AsP)^{+\cdot}$), and others.

## Synthesis of $(OC)_5W(AsP)(C_6H_{10})_2$, 9-$W(CO)_5$

To a thawing solution of [Na(THF)][$(OC)_5$WAs≡Nb(N[Np]Ar)$_3$] ([Na(THF)][**3**-$W(CO)_5$], 0.200 g, 0.173 mmol) in $Et_2O$ (7 mL) was added dropwise a thawing $Et_2O$ (5 mL) solution of Mes*NPCl (0.057 g, 0.175 mmol, 1 eq). After 30 s of stirring, 200 $\mu$L (1.77 mmol, 10.2 eq) of 2,3-dimethyl-1,3-butadiene was added *via* syringe. The dark red reaction mixture was stirred for 1 h and then pumped down to dryness, leaving behind a dark red residue. The residue was extracted with 10 mL of toluene and filtered through Celite to remove NaCl. The red filtrate was evaporated to dryness and 5 mL of acetonitrile was added, resulting in precipitation of a yellow solid. The yellow solid was isolated by filtration, and characterized as the niobium imido complex, (Mes*N)Nb-(N[Np]Ar)$_3$ (**5**, 0.159 g, 0.172 mmol, 99% yield). The red-brown filtrate was evaporated to dryness and slurried in 2 mL of *n*-pentane. Diethyl ether was added dropwise to the slurry until all solids present dissolved and the mixture was placed in the freezer for 48 h at −35 °C. Colorless, X-ray quality crystals of **9**-$W(CO)_5$ were isolated by filtration and washed with 1 mL of cold *n*-pentane. Total yield: 0.018 g, 0.030 mmol, 17%. Note: Monitoring formation of **9**-$W(CO)_5$ via $^{31}$P NMR ($PPh_3$ as internal standard) gave an overall yield of 53%. Elem. Anal. Calcd. for $C_{17}H_{20}O_5PAsW$: C, 34.37; H, 3.39. Found: C, 33.92; H 3.32. $^1$H NMR (benzene-$d_6$, 20 °C, 400 MHz): $\delta$ = 2.25 (m, 2H), 2.05 (d, 2H), 1.70 -1.57 (m, 4H), 1.55 (bs, 6H, C$H_3$), 1.38 (dd, $J$ = 5 Hz and 1Hz, 6H, C$H_3$) ppm. $^{13}$C{$^1$H} NMR (benzene-$d_6$, 20 °C, 100.6 MHz): $\delta$ = 199.9 (d, $J_{CP}$ = 23 Hz, *trans* *C*O), 197.7 (d, $J_{CP}$ = 6.5 Hz, $J_{CW}$ = 125 Hz, *cis* *C*O), 124.3 (d, $J_{CP}$ = 8 Hz, *C*$CH_3$), 33.8 (bs), 26.6 (d, $J_{CP}$ = 6 Hz), 21.4 (d, $J_{CP}$ = 2 Hz), 20.8 (d, $J_{CP}$ = 3 Hz) ppm. $^{31}$P{$^1$H} NMR (benzene-$d_6$, 20 °C, 121.5 MHz): $\delta$ = −12 (s, $J_{WP}$ = 225 Hz) ppm. FTIR (KBr windows, thin film): 2916(w), 2857(w), 2354(w), 2065(s), 1975(s), 1950(s), 1898(vs), 1645(w), 1436(w), 1408(w), 1383(w), 1048(w), 1018(w), 830(m), 819(m), 808(w), 780(w), 597(s), 575(vs) cm$^{-1}$. HRMS-EI: Calcd. for $M^{+\cdot}$: 593.978. Found: 593.980. Also present: 565.984 ($W(CO)_4(AsP)(C_6H_{10})_2^{+\cdot}$), 483.906 ($W(CO)_4(AsP)(C_6H_{10})^{+\cdot}$), 429.822 ($W(CO)_5(AsP)^{+\cdot}$), 401.827 ($W(CO)_4(AsP)^{+\cdot}$), and others.

## Kinetics of the Fragmentation of 4

Stock solutions containing ($\eta^2$-AsPNMes*)Nb(N[Np]Ar)$_3$ (**4**, 151 mg) and ONb(N[Np]Ar)$_3$ (46 mg, used as an internal standard) were prepared in $C_6D_6$ (4.1 g) and stored at $-35$ °C between uses. An aliquot of this solution was transferred to a sealable (J. Young) NMR tube, which was then inserted into a pre-warmed NMR probe (60 °C). The temperature of the probe was verified by an ethylene glycol NMR thermometer before each run. Four-scan $^1$H NMR spectra (relaxation delay = 16 s) were collected every three minutes over a period of three half-lives. The integral of the methylene residue of **4** as a function of time, corrected versus the internal standard, was fit to the first-order rate equation, $I(t) = Ae^{-kt} + b$, using the automated routine of Origin 6.[48] The experiment was repeated three times. The average rate constant for the decay of **4** at 60 °C is 2.9(1) $\times$ $10^{-4}$ $s^{-1}$. As shown in Figure S22, conversion of **4** to the niobium imido complex, (Mes*N)Nb(N[Np]Ar)$_3$ (**5**), is not quantitative and other unidentified anilide-containing products are also formed.

## Kinetics of the Fragmentation of 4-W(CO)$_5$

A thawing $Et_2O$ solution (1 mL) of Mes*NPCl (17 mg, 0.052 mmol, 1 equiv) was added to a thawing $Et_2O$ solution (2 mL) of [Na(THF)][(OC)$_5$WAs≡Nb(N[Np]Ar)$_3$] ([Na(THF)][**3**-W(CO)$_5$], 58 mg, 0.050 mmol). This solution was stirred for 30 s before the solvent was removed *in vacuo*. The residue was extracted with a toluene-$d_8$ (1.0 g) solution of ferrocene (7 mg, 0.04 mmol, used as an internal standard). The resulting extract was filtered cold through Celite into a sealable (J. Young) NMR tube, which was then frozen for transport to an NMR probe pre-cooled to 10 °C. The temperature of the probe was verified by an ethylene glycol NMR thermometer before each run. Four-scan $^1$H NMR spectra (relaxation delay = 16 s) were collected every three minutes over a period of four half-lives. The integral of the methylene residue of **4**-W(CO)$_5$ as a function of time, corrected versus the internal standard, was fit to the first-order rate equation, $I(t) = Ae^{-kt} + b$, using the automated routine of Origin 6.[48] The experiment was repeated three times.[49] The average rate constant for the decay of **4**-W(CO)$_5$ at 10 °C is 5.5(3) $\times$ $10^{-4}$ $s^{-1}$. As shown in Figure S23,

conversion of **4**-$W(CO)_5$ to the niobium imido complex, (Mes*N)Nb(N[Np]Ar)$_3$ (**5**), is nearly quantitative.

## Details of X-ray Structure Determinations

Crystals were mounted in hydrocarbon oil on a nylon loop or a glass fiber. Low-temperature (100 K) data were collected on a Siemens Platform three-circle diffractometer coupled to a Bruker-AXS Smart Apex CCD detector with graphite-monochromated Mo K$\alpha$ radiation ($\lambda$ = 0.71073 Å) performing $\phi$- and $\omega$-scans. A semi-empirical absorption correction was applied to the diffraction data using SADABS.[50] All structures were solved by direct or Patterson methods using SHELXS[51,52] and refined against $F^2$ on all data by full-matrix least squares with SHELXL-97.[52,53] All non-hydrogen atoms were refined anisotropically. All hydrogen atoms were included in the model at geometrically calculated positions and refined using a riding model. The isotropic displacement parameters of all hydrogen atoms were fixed to 1.2 times the $U$ value of the atoms to which they are linked (1.5 times for methyl groups). In structures where disorders were present, the disorders were refined within SHELXL with the help of rigid bond restraints as well as similarity restraints on the anisotropic displacement parameters for neighboring atoms and on 1,2- and 1,3-distances throughout the disordered components. The relative occupancies of disordered components were refined freely within SHELXL.[54] Further details on all structures are provided in Tables S1 and S2, and in the form of cif files available as part of the Supporting Information or from the CCDC under deposition numbers 710856-710861.[55]

## Computational Details

Quantum chemical calculations were carried out to probe the electronic structure of the As—As and As—P bonds contained within the new product molecules, to be compared with some reference systems analyzed by the same methods. Geometry optimizations were carried out using the Amdsterdam Density Functional (ADF) code version 2006.01,[56] using the LDA functional of Vosko, Wilk, and Nusair (VWN)[57] together with the GGA functional known as OLYP which is

a combination of Handry and Cohen's OPTX functional for exchange and Lee, Yang, and Parr's nonlocal correlation functional.[58] The zero-order regular approximation (ZORA) was used for inclusion of relativistic effects.[59] The basis sets were QZ4P (quadruple-$\zeta$ with four polarization functions) for As, P, Nb, TZ2P for C, N, W, and O and DZP for H atoms as supplied with ADF, and frozen core approximations were made for carbons on the anilide ligands (1s). All molecules were geometry-optimized without symmetry constraints to default convergence criteria and energies are uncorrected for zero-point energies. Bond multiplicities were calculated using the method of Nalewajski and Mrozek within ADF.[60] Electron density topologies and orbital contours were analyzed using the packages DGrid and Basin by Kohout.[61]

## Acknowledgement

We gratefully acknowledge the US National Science Foundation for support of this research through grant CHE-719157 and through a predoctoral fellowship to N. A. P. This work was also supported by the Natural Sciences and Engineering Research Council (NSERC) of Canada through a post-doctoral fellowship to H. A. S. We would also like to thank Prof. Dr. Karsten Meyer for a generous gift of the $As_4$-generating apparatus.

## Supporting Information Available

Additional experimental details and figures showing NMR spectra, variable-temperature NMR data, mass spectra, kinetic plots, and X-ray crystallography structures; tables of crystal data; lists of optimized geometry coordinates; and crystallographic information files in CIF format. This material is available free of charge via the Internet at http://pubs.acs.org.

## References

(1) Rodionov, A.; Kalendarev, R.; Eiduss, J.; Zhukovskii, Y. *J. Mol. Struct.* **1996**, *380*, 257–266.

(2) Bettendorff, A. *Annalen Chem. Pharm.* **1867**, *144*, 110–114.

(3) Linck, G. E. *Chem. Ber.* **1899**, *32*, 881–897.

(4) Stock, A.; Siebert, W. *Chem. Ber.* **1905**, *38*, 966–968.

(5) Erdmann, H.; von Unruh, M. *Z. Anorg. Chem.* **1902**, *32*, 437–452.

(6) Scherer, O. J.; Sitzmann, H.; Wolmershäuser, G. *J. Organomet. Chem.* **1986**, *309*, 77–86.

(7) (a) Scherer, O. J.; Sitzmann, H.; Wolmershäuser, G. *Angew. Chem. Int. Ed. Engl.* **1989**, *28*, 212–213; (b) Scherer, O. J.; Wiedemann, W.; Wolmershäuser, G. *J. Organomet. Chem.* **1989**, *361*, C11–C14; (c) Scherer, O. J.; Vondung, J.; Wolmershäuser, G. *J. Organomet. Chem.* **1989**, *376*, C35–C38; (d) Scherer, O. J.; Blath, C.; Wolmershäuser, G. *J. Organomet. Chem.* **1990**, *387*, C21–C24; (e) Scherer, O. J.; Wiedemann, W.; Wolmershäuser, G. *Chem. Ber.* **1990**, *123*, 3–6; (f) Scherer, O. J.; Winter, R.; Heckmann, G.; Wolmershäuser, G. *Angew. Chem. Int. Ed. Engl.* **1991**, *30*, 850–852; (g) Scherer, O. J.; Blath, C.; Heckmann, G.; Wolmershäuser, G. *J. Organomet. Chem.* **1991**, *409*, C15–C18; (h) Scherer, O. J. *Acc. Chem. Res.* **1999**, *32*, 751–762.

(8) (a) Scherer, O. J.; Braun, J.; Wolmershäuser, G. *Chem. Ber.* **1990**, *123*, 471–475; (b) Scherer, O. J.; Braun, J.; Walther, P.; Wolmershäuser, G. *Chem. Ber.* **1992**, *125*, 2661–2665; (c) Scherer, O. J.; Kemény, G.; Wolmershäuser, G. *Chem. Ber.* **1995**, *128*, 1145–1148.

(9) (a) Di Vaira, M.; Ghilardi, C. A.; Midollini, S.; Sacconi, L. *J. Am. Chem. Soc.* **1978**, *100*, 2550–2551; (b) Di Vaira, M.; Midollini, S.; Sacconi, L.; Zanobini, F. *Angew. Chem. Int. Ed. Engl.* **1978**, *17*, 676–677.

(10) (a) Tan, R. P.; Comerlato, N. M.; Powell, D. R.; West, R. *Angew. Chem. Int. Ed. Engl.* **1992**, *31*, 1217–1218; (b) Fanta, A. D.; Tan, R. P.; Comerlato, N. M.; Driess, M.; Powell, D. R.; West, R. *Inorg. Chim. Acta* **1992**, *198-200*, 733–739.

(11) Figueroa, J. S.; Cummins, C. C. *J. Am. Chem. Soc.* **2003**, *125*, 4020–4021.

(12) Figueroa, J. S.; Cummins, C. C. *Angew. Chem. Int. Ed.* **2004**, *43*, 984–988.

(13) (a) Figueroa, J. S.; Cummins, C. C. *J. Am. Chem. Soc.* **2004**, *126*, 13916–13917; (b) Figueroa, J. S.; Cummins, C. C. *Angew. Chem. Int. Ed.* **2005**, *44*, 4592–4596; (c) Figueroa, J. S.; Cummins, C. C. *Dalton Trans.* **2006**, 2161–2168.

(14) Niecke, E.; Nieger, M.; Reichert, F. *Angew. Chem. Int. Ed. Engl.* **1988**, *27*, 1715–1716.

(15) Piro, N. A.; Figueroa, J. S.; McKellar, J. T.; Cummins, C. C. *Science* **2006**, *313*, 1276–1279.

(16) Piro, N. A.; Cummins, C. C. *J. Am. Chem. Soc.* **2008**, *130*, 9524–9535.

(17) Piro, N. A.; Cummins, C. C. *Inorg. Chem.* **2007**, *46*, 7387–7393.

(18) Cossairt, B. M.; Diawara, M.-C.; Cummins, C. C. *Science* **2009**, *323*, 602.

(19) Ugai, Y. A.; Semenova, G. V.; Berendt, E.; Goncharov, E. G. *Russ. J. Phys. Chem.* **1979**, *53*, 576–577.

(20) Karakaya, I.; Thompson, W. T. *J. Phase Equilib.* **1991**, *12*, 343–6.

(21) Yee, K. K.; Jones, W. E. *J. Chem. Soc. D., Chem. Commun.* **1969**, 586a.

(22) Leung, F.; Cooke, S. A.; Gerry, M. C. L. *J. Mol. Spectrosc.* **2006**, *238*, 36–41.

(23) Gingerich, K. A.; Cocke, D. L.; Kordis, J. *J. Phys. Chem.* **1974**, *78*, 603–606.

(24) (a) Davies, J. E.; Kerr, L. C.; Mays, M. J.; Raithby, P. R.; Tompkin, P. K.; Woods, A. D. *Angew. Chem. Int. Ed.* **1998**, *37*, 1428–1429; (b) Davies, J. E.; Mays, M. J.; Raithby, P. R.; Shields, G. P.; Tompkin, P. K.; Woods, A. D. *J. Chem. Soc., Dalton Trans.* **2000**, 1925–1930.

(25) Herrmann, W. A.; Koumbouris, B.; Zahn, T.; Ziegler, M. L. *Angew. Chem. Int. Ed. Engl.* **1984**, *23*, 812–814.

(26) Fenske, D.; Fleischer, H.; Persau, C. *Angew. Chem. Int. Ed. Engl.* **1989**, *28*, 1665–1667.

(27) DiMaio, A.-J.; Baldacchini, C. J.; Rheingold, A. L. *Acta Crystallogr., Sect. C: Cryst. Struct. Commun.* **1990**, *46*, 492–494.

(28) Pyykkö, P.; Atsumi, M. *Chem. Eur. J.* **2009**, *15*, 186–197.

(29) Pyykkö, P.; Atsumi, M. **2009**, Submitted for publication.

(30) Chen, H.; Olmstead, M. M.; Pestana, D. C.; Power, P. P. *Inorg. Chem.* **1991**, *30*, 1783–1787.

(31) Bouslikhane, M.; Gornitzka, H.; Escudie, J.; Ranaivonjatovo, H. *J. Organomet. Chem.* **2001**, *619*, 275–279.

(32) Hirsch, A.; Chen, Z.; Jiao, H. *Angew. Chem. Int. Ed.* **2001**, *40*, 2834–2838.

(33) Maxwell, L. R.; Hendricks, S. B.; Mosley, V. M. *J. Chem. Phys.* **1935**, *3*, 699–709.

(34) Please see Supporting Information.

(35) Scheer, M.; Müller, J.; Häser, M. *Angew. Chem. Int. Ed. Engl.* **1996**, *35*, 2492–2496.

(36) Mösch-Zanetti, N. C.; Schrock, R. R.; Davis, W. M.; Wanninger, K.; Seidel, S. W.; O'Donoghue, M. B. *J. Am. Chem. Soc.* **1997**, *119*, 11037–11048.

(37) (a) Gascoin, F.; Sevov, S. C. *Angew. Chem. Int. Ed.* **2002**, *41*, 1232–1234; (b) Gascoin, F.; Sevov, S. C. *Inorg. Chem.* **2003**, *42*, 904–907; (c) Gascoin, F.; Sevov, S. C. *Inorg. Chem.* **2003**, *42*, 8567–8571.

(38) Pyykkö, P.; Riedel, S.; Patzschke, M. *Chem. Eur. J.* **2005**, *11*, 3511–3520.

(39) Cowley, A. H.; Lasch, J. G.; Norman, N. C.; Pakulski, M.; Whittlesey, B. R. *J. Chem. Soc., Chem. Commun.* **1983**, 881–882.

(40) Schinkels, B.; Ruban, A.; Nieger, M.; Niecke, E. *Chem. Commun.* **1997**, 293–294.

(41) Brask, J. K.; Fickes, M. G.; Sangtrirutnugul, P.; Durà-Vilà, V.; Odom, A. L.; Cummins, C. C. *Chem. Commun.* **2001**, 1676–1677.

(42) Agarwal, P.; Piro, N.; Meyer, K.; Müller, P.; Cummins, C. *Angew. Chem. Int. Ed.* **2007**, *46*, 3111–3114.

(43) As commented by a reviewer, the trapping of the AsP fragment with the dienes is somewhat tenuous, since it is based solely on the NMR shift obtained in a mixture of compounds.

(44) Cherry, J.-P.; Stephens, F. H.; Johnson, M. J. A.; Diaconescu, P. L.; Cummins, C. C. *Inorg. Chem.* **2001**, *40*, 6860–6862.

(45) Stephens, F. H.; Johnson, M. J. A.; Cummins, C. C.; Kryatova, O. P.; Kryatov, S. V.; Rybak-Akimova, E. V.; McDonough, J. E.; Hoff, C. D. *J. Am. Chem. Soc.* **2005**, *127*, 15191–15200.

(46) Umbarkar, S.; Sekar, P.; Scheer, M. *J. Chem. Soc., Dalton Trans.* **2000**, 1135–1137.

(47) Esterhuysen, C.; Frenking, G. *Chem. Eur. J.* **2003**, *9*, 3518–3529.

(48) http://microcal.com, Microcal(TM) Origin Version 6.0, Copyright 1991-1999, Microcal Software, Inc.

(49) It should be noted that by the time data collection started on the samples, approximately one third of the **4**-$W(CO)_5$ present in solution had already converted to the niobium imido **5**.

(50) Sheldrick, G. M. *SADABS*; Bruker AXS Inc., 2005.

(51) Sheldrick, G. M. *Acta Crystallogr., Sect. A: Found. Crystallogr.* **1990**, *46*, 467–473.

(52) Sheldrick, G. M. *Acta Crystallogr., Sect. A: Found. Crystallogr.* **2008**, *64*, 112–122.

(53) Sheldrick, G. M. *SHELXL-97*; University of Göttingen, 1997.

(54) Müller, P.; Herbst-Irmer, R.; Spek, A. L.; Schneider, T. R.; Sawaya, M. R. *Crystal structure refinement: A crystallographer's guide to SHELXL*; Oxford University Press: Oxford, 2006.

(55) This material is available free of charge at http://www.ccdc.cam.ac.uk/data_request/cif.

(56) (a) te Velde, G.; Bickelhaupt, F. M.; Baerends, E. J.; Guerra, C. F.; van Gisbergen, S. J. A.; Snijders, J. G.; Ziegler, T. *J. Comput. Chem.* **2001**, *22*, 931–967; (b) http://www.

scm.com, ADF2006.01, SCM, Theoretical Chemistry, Vrije Universiteit, Amsterdam, The Netherlands.

(57) Vosko, S. H.; Wilk, L.; Nusair, M. *Can. J. Phys.* **1980**, *58*, 1200–1211.

(58) (a) Lee, C.; Yang, W.; Parr, R. G. *Phys. Rev. B* **1988**, *37*, 785–789; (b) Handry, N. C.; Cohen, A. J. *Mol. Phys.* **2001**, *99*, 403–412; (c) Baker, J.; Pulay, P. *J. Comput. Chem.* **2003**, *24*, 1184–1191.

(59) (a) van Lenthe, E.; Baerends, E. J.; Snijders, J. G. *J. Chem. Phys.* **1993**, *99*, 4597–4610; (b) van Lenthe, E.; Baerends, E. J.; Snijders, J. G. *J. Chem. Phys.* **1994**, *101*, 9783–9792; (c) van Lenthe, E.; Ehlers, A.; Baerends, E.-J. *J. Chem. Phys.* **1999**, *110*, 8943–8953.

(60) Michalak, A.; DeKock, R. L.; Ziegler, T. *J. Phys. Chem. A* **2008**, *112*, 7256–7263.

(61) Kohout, M. *DGrid*, 2008.

# Graphical TOC Entry